Supporting Information for

Efficient Photoreforming of Biomass Derived 5-(Hydroxymethyl)furfural and Simultaneous Green Hydrogen Production by Defective Graphitic Carbon Nitride Photocatalysts

Thi Kim Anh Nguyen[a], Thành Trần-Phú[a,g], Xuan Minh Chau Ta[a], Biswaranjan Mohanty[b], Jodie A. Yuwono[c], Silvia Nappini[d], Ilargi Napal Azcona[d,e], Qi Wang[a], Anita Ho-Baillie[f], Christopher G. Bailey[f], Elena Magnano[c], Antonio Tricoli[a*]*

[a] Nanotechnology Research Laboratory, Faculty of Engineering, University of Sydney, NSW 2006, Australia
[b] Sydney Analytical, The University of Sydney, Sydney, NSW 2006, Australia
[c] School of Chemical Engineering, The University of Adelaide, Adelaide, Australia
[d] IOM-CNR Istituto Officina dei Materiali AREA Science Park Basovizza, Trieste 34149, Italy
[e] Universitá degli Studi di Trieste, Physics Department, P.le Europa 1, 34127, Trieste, Italy
[f] School of Physics, The University of Sydney, Sydney, New South Wales 2006, Australia
[g] School of Science, Computing and Engineering Technologies, Swinburne University of Technology, Hawthorn, Victoria 3122, Australia

Corresponding Authors:

*E-mails: antonio.tricoli@sydney.edu.au
thanhtran@swin.edu.au

Table of contents

HMF adsorption test: 100 mg of catalyst was added to 50 mL of a 5 mM HMF solution and stirred for 2 hours. The resulting mixture was then centrifuged at 4000 rpm for 1 hour. The supernatant was collected and filtered through a 0.2 μm polytetrafluoroethylene (PTFE) membrane filter (Whatman GmbH, Dassel, Germany). The filtrate was subsequently analysed using proton nuclear magnetic resonance (^{1}H NMR) spectroscopy. For NMR analysis, 600 μL of each sample was prepared in a solvent mixture containing 95% H_2O and 5% D_2O (v/v), spiked with 0.1 mM non-deuterated DMSO. D_2O served as the NMR lock solvent, while DMSO was used as internal standards for quantification and chemical shift calibration. Samples were loaded into standard 5 mm NMR tubes for data acquisition. ^{1}H NMR spectra (1D, pulse sequence: zgesgppe) were recorded on a Bruker AVANCE III 800 MHz spectrometer at 25 °C equipped with a Z-gradient triple-resonance CryoProbe with inverse detection (TCI). Spectra were acquired with a time domain (TD) of 64k complex points and 512 scans, using a relaxation delay of 10 s. Prior to Fourier transformation, an exponential window function with a line broadening (LB) of 0.3 Hz was applied. Data collection, processing, and analysis were performed using TopSpin 3.7 software (Bruker Biospin). Chemical shifts were referenced to the DMSO peak at 2.568 ppm.

Synthesis of nickel loading on CN: Nickel as a co-catalyst was deposited by a photodeposition method following procedure of Pt loading as described in **Experimental Section**. As-synthesised etched CN (100 mg) was added in reactor and dispersed in 50 mL of water with 10 vol% of TEOA then stirred for 10 min at 300 rpm. After that, Ni precursor solution (6 wt% Pt) was added and stirred for 30 min at 300 rpm under saturated argon (Ar) (100 ml min^{-1}). The mixture then was irradiated under solar simulator (AM 1.5 G, 100 mW cm^{-2}, 23 ± 2 °C) with Ar purging (20 ml min^{-1}) for 15 hours. Obtained nickel-loaded etched CN is labelled as etched Ni/CN. For powder collection, suspension was centrifuged for 4000 rpm in 3 hours to remove access water. Obtained solid sample was placed in liquid nitrogen for 20 min before freeze drying in 15 hours.

Solid-state NMR sample preparation: 100 mg of Pt-loaded catalyst was dispersed in 100 mL of a 10 mM HMF solution and stirred for 1 h at 300 rpm. Although the reaction conditions in this work use 5 mM HMF, this concentration was too low for reliable NMR detection; therefore, a 10 mM solution was chosen. After adsorption, the suspension was centrifuged at 4000 rpm for 3 h to remove excess water, and the recovered solid was frozen in liquid nitrogen for 20 min before freeze-drying for 15 h. A fresh photocatalyst without HMF exposure was also measured as a reference.

Solid-state NMR measurement: 1D ^{1}H solid-state NMR spectra (rotor-synchronized echomas pulse sequence with asymmetry in delays before/after π pulse) were collected on a Bruker AVANCE III Ascend widebore 400 MHz spectrometer equipped with a PH MAS DVT 400W1 BL4 N-P/H probe. All the solid samples were packed in a 4 mm rotor, and a MAS rate of 14 kHz was used. Data acquisition and processing were carried out using Topspin v3.7 (Bruker Biospin).

Charge closure calculation: Charge balance calculation was conducted by linking H_2 evolution to the key quantified oxidation products, namely DFF, FFCA and CO_2 as products as follows. Each H_2 molecule corresponds to 2 electrons consumed. The oxidation of HMF to DFF and FFCA generates 2 and 4 electrons, respectively. HMF oxidation to CO_2 correspond to 4 electrons per CO_2 formed:

Oxidation haft-reactions

Primary oxidation of HMF to DFF involves dehydrogenation of one alcohol group (-CH_2OH) into an aldehyde group (-CHO):

$$HMF \rightarrow DFF + 2H^+ + 2e^-$$

Further oxidation of DFF into FFCA involves the transformation of one aldehyde group (-CHO) into a carboxylic acid group (-COOH) via hydration and dehydrogenation:

$$DFF + H_2O \rightarrow FFCA + 2H^+ + 2e^-$$

Photooxidation of HMF ($C_6H_6O_3$) to CO_2 can be described as:

$$C_6H_6O_3 + 9H_2O \rightarrow 6CO_2 + 24H^+ + 24e^-$$

Reduction half-reaction

$$2H^+ + 2e^- \rightarrow H_2$$

Charge balance closure is calculated as follow:

$$\% \, closure = \frac{n_{e^-}^{ox}}{n_{e^-}^{red}}$$

Where $n_{e^-}^{ox}$ is the number of electrons generated from the HMF photooxidation, and $n_{e^-}^{red}$ is the number of electrons required for the photoreduction of water.

According to the products concentrations measured after 24 hours of HMF photoreforming:

$n_{e^-}^{red} =$ $2n_{H2\ measured} = 2\times0.1247 = 0.2494$ mmol (from GC-TCD analysis).

$n_{e^-}^{ox} =$ $2n_{H2\ products} = 2n_{(DFF)} + 4n_{(FFCA)} + 4n_{(CO2)} = 2\times0.0386 + 4\times0.0292 + 4\times0.0130 = 0.2460$ mmol (from ^{1}H NMR for DFF and FFCA and GC-FID analysis for CO_2).

Our calculations indicate a charge balance closure of 98.64 %. The residual 1.36 % of H_2 measured is likely due to the oxidation of minor products that could not be quantified in this study.

HMF photoreforming in D_2O: after the platinum photodeposition step, suspension was centrifuged for 4000 rpm in 1 hour to remove access water. The obtained solid sample was placed in liquid nitrogen for 20 min before freeze drying in 15 hours for etched Pt/CN powder collection. 100 mg of etched Pt/CN powder and 50 ml of D_2O were added in reactor stirred for 10 min at 300 rpm. 50 ml of HMF 10 mM (in D_2O based) was added into reaction cell and the final HMF concentration for measurement is 5 mM. The suspension was purged with argon (Ar) (100 ml min^{-1}) in the dark for 30 min and stirred at 400 rpm. Before initiating the photoreaction, an online gas chromatograph (Shimadzu Nexis GC-2030 Series) analysis is used to verify the absence of oxygen and ensure the airtightness of the photocatalytic systems. Finally, the reaction cell is illuminated under solar simulator irradiation using Ar as the carrier gas (20 mL min^{-1}) and stirred at 400 rpm while the reaction temperature was maintained at 23 ± 2 ºC.

The apparent energy consumption (AEC) for each product was estimated based on the ratio of the total input irradiation energy to the number of moles of product formed. The irradiation energy was calculated from the lamp power (P, W h), illuminated area (A = 28 cm^2) and the illumination time (t, h), according to:

$$E_{input} = P \times t = I \times A \times t =$$ 0.100 W cm^{-2} × 28 cm^2 × 24 h = 0.0672 kWh

The energy consumption per mole of product (AEC, kWh mol^{-1}) is expressed as:

$$AEC = \frac{E_{input}}{n_{product}}$$

where $n_{product}$ is the number of moles of H_2, DFF, or FFCA produced. The results are summarised in ***Table S2***.

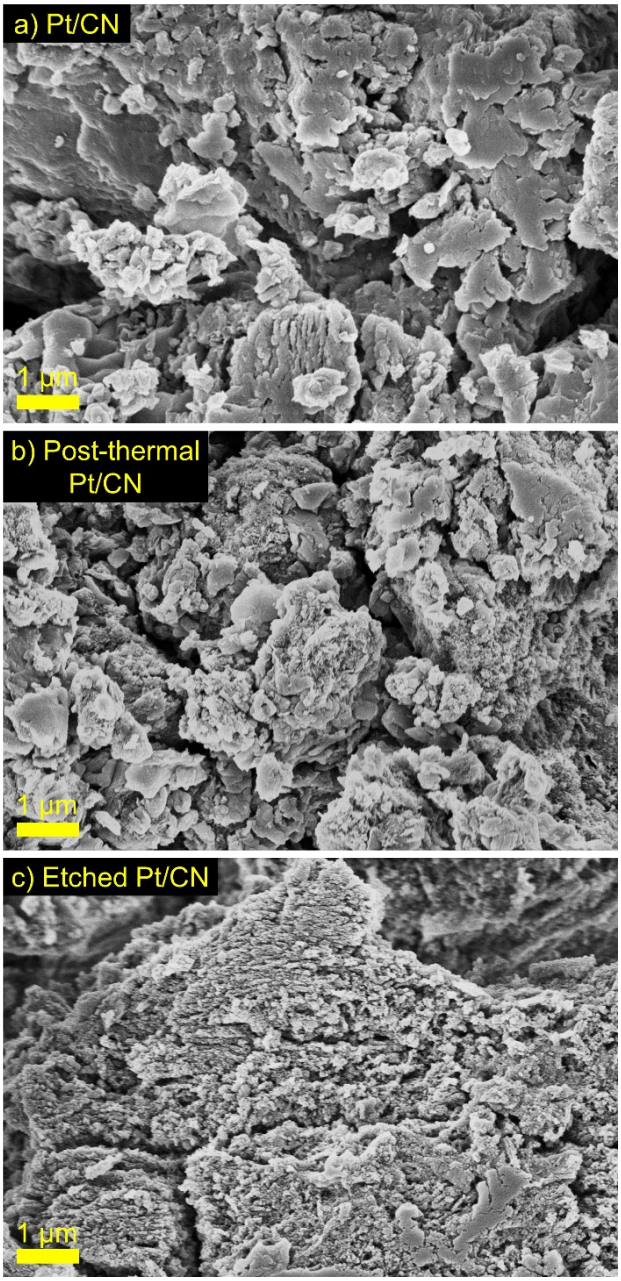

Figure S1. SEM image of CN. Bulk Pt/CN exhibits large, layered assemblies with an uneven size distribution (**Figure S1a**). After thermal treatment, the bulky layered structure of CN transforms into a thinner, smaller form with numerous pores resulting from gas release during melamine decomposition **(Figure S1b).** This post-thermal etching process also leads to a mass loss, as reflected by the mass decrease between Pt/CN and post-thermal Pt/CN, consistent with the TGA results. The formation of pores can be seen as imperfections in the CN layers, which enhance edge contact for subsequent chemical treatments. Chemical functionalization further thins the lamellar structure and induces larger interconnected pores in the etched Pt/CN sample, enhancing its catalytic performance.

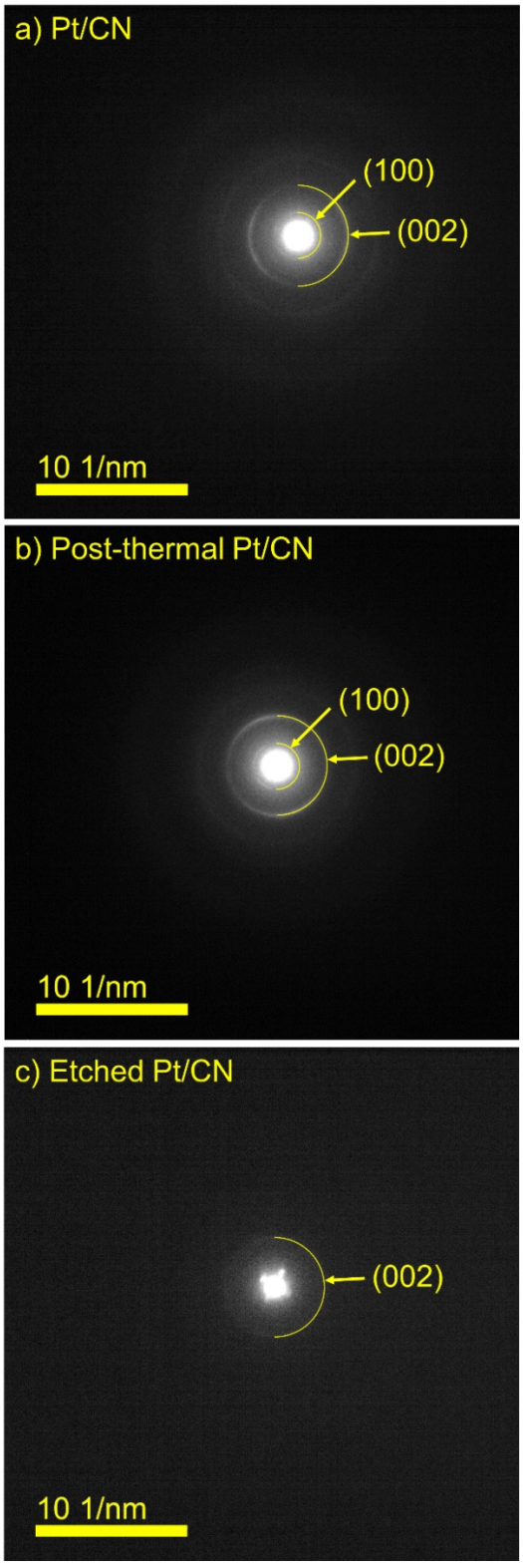

Figure S2. Detailed SAED patterns of CN samples from TEM analysis.

(a) bulk Pt/CN, (b) post-thermal Pt/CN and (c) etched Pt/CN. SAED patterns of all CN samples exhibit similar brilliant rings, showing diffraction patterns of the main (002) plane with a lattice space of around 3.07 Å for Pt/CN, slightly smaller number of 3.10 Å for post-thermal Pt/CN and 3.12 Å for etched Pt/CN. While Pt/CN and post-thermal Pt/CN shows two bright rings, etched Pt/CN exhibits only evident rings of (002) plane. SAED confirms that the Pt/CN and post-thermal have a greater level of crystallinity.

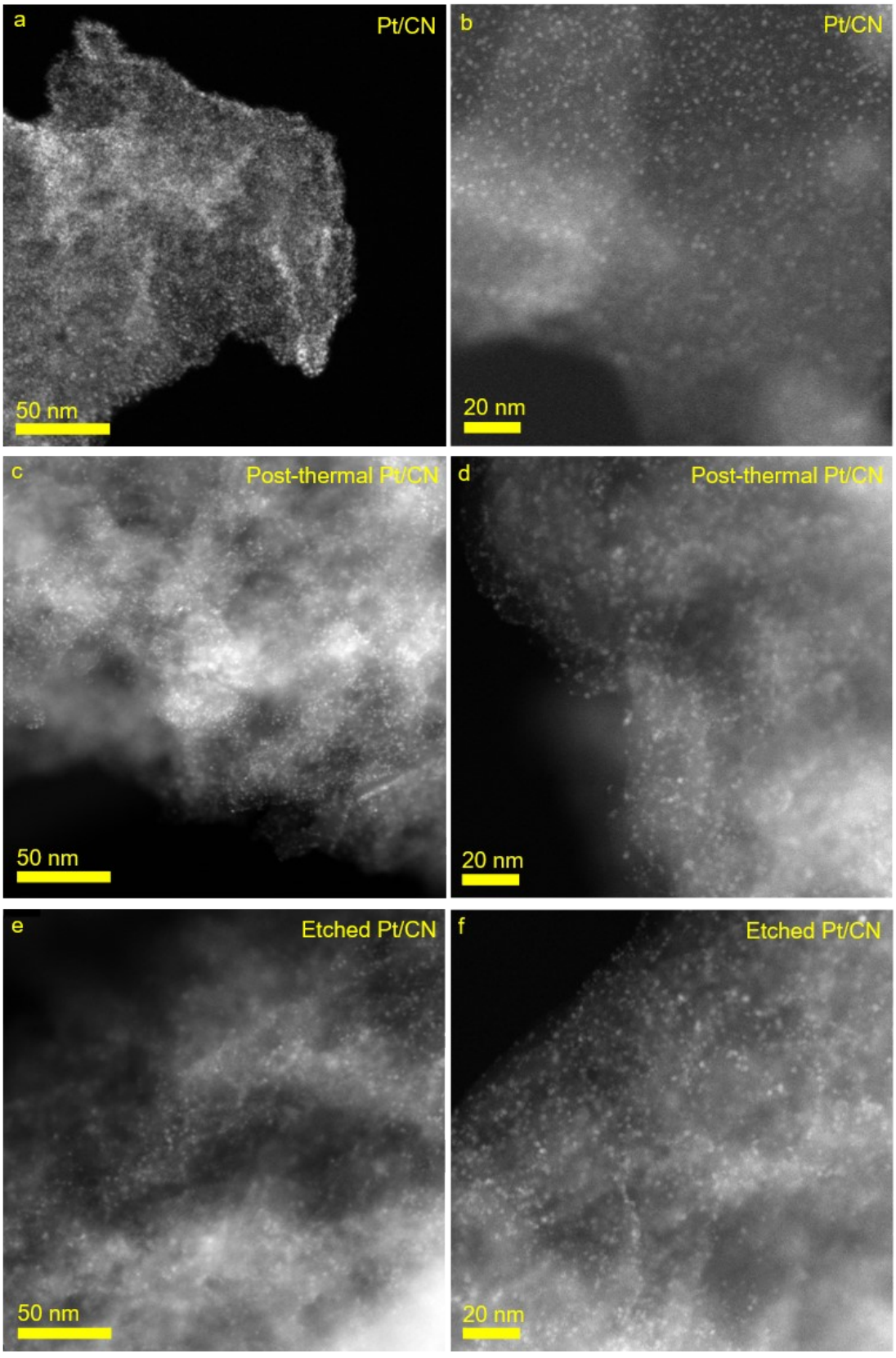

Figure S3. HR-TEM images of (a, b) Pt/CN, (c, d) post-thermal Pt/CN and (e, f) etched Pt/CN

Table S1. Pt concentration remaining in solution after HMF photoreforming via ICP-MS.

Samples	Pt wt% after 8 h	Pt wt% after 24 h	Pt wt% after 2 days	Pt wt% after 3 days	Pt wt% after 5 days
	Unwashed catalyst after Pt photodeposition		Catalyst was washed after Pt photodeposition		
Pt/CN	0.35	0.26	-	-	-
Post-thermal Pt/CN	0.38	0.17	-	-	-
Etched Pt/ECN	0.25	0.14	LoD	LoD	LoD

LoD: Low of detection.

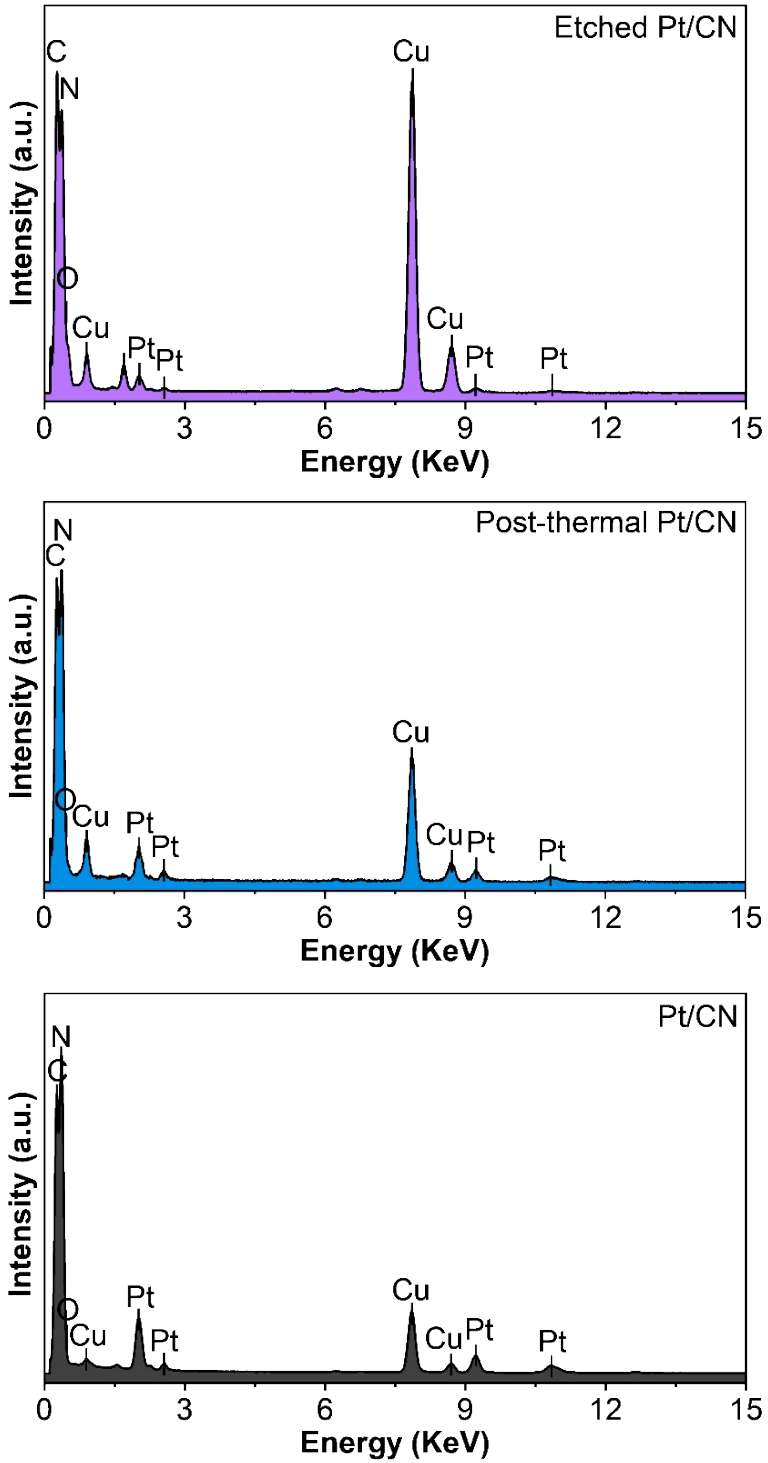

Figure S4. EDX elemental mapping analysis of CN. It clearly indicates that carbon, nitrogen, oxygen, and platinum components are main components in all CN samples. The peak of Cu belongs to sample holders.

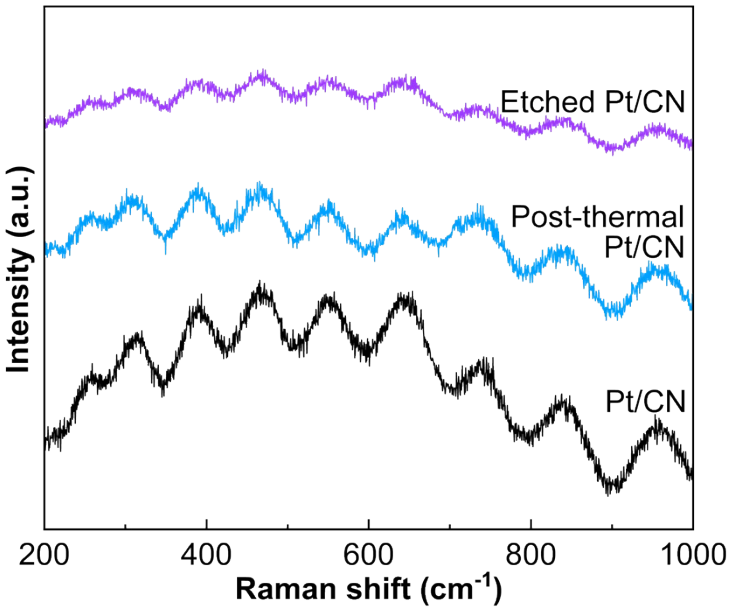

Figure S5. Raman spectra of CN. There are no peaks observed in Raman spectra.

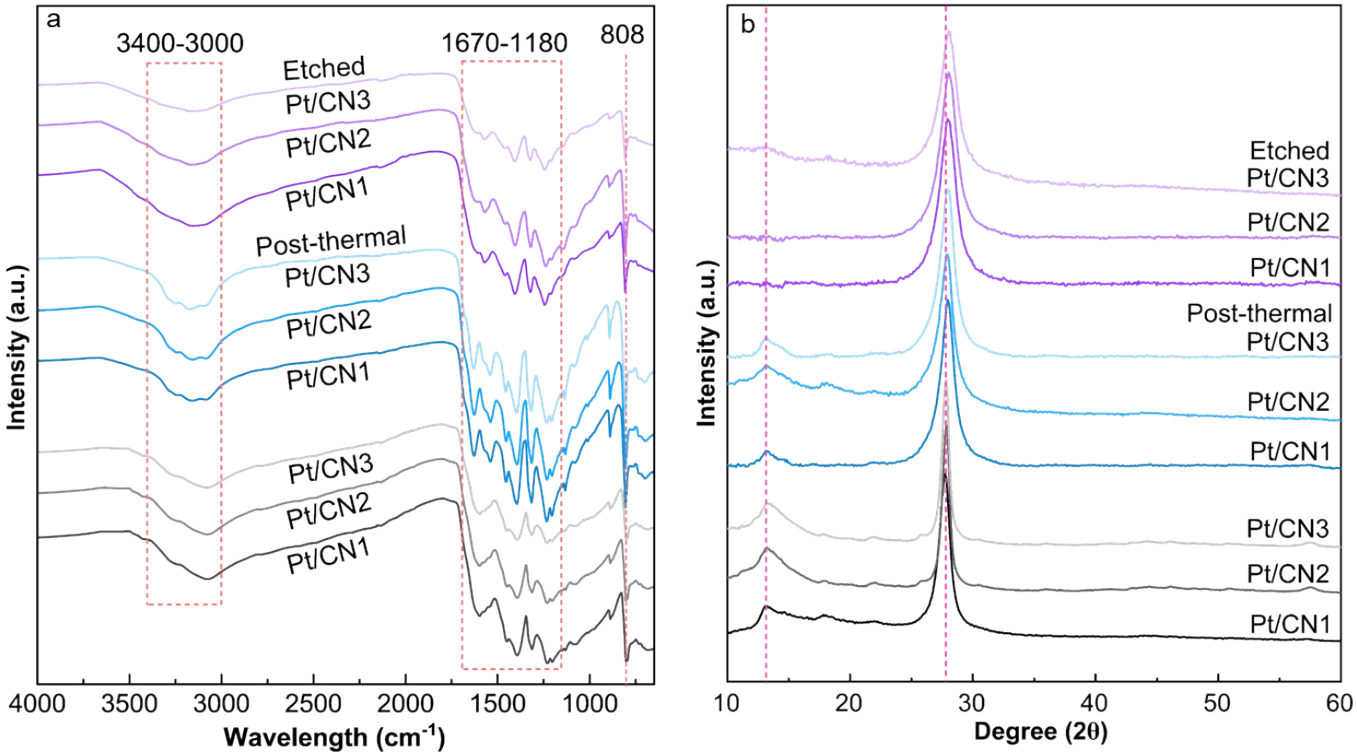

Figure S6. (a) FT-IR spectra and (b) X-ray diffraction of bulk Pt/CN (black), post-thermal Pt/CN (blue), etched Pt/CN (purple).

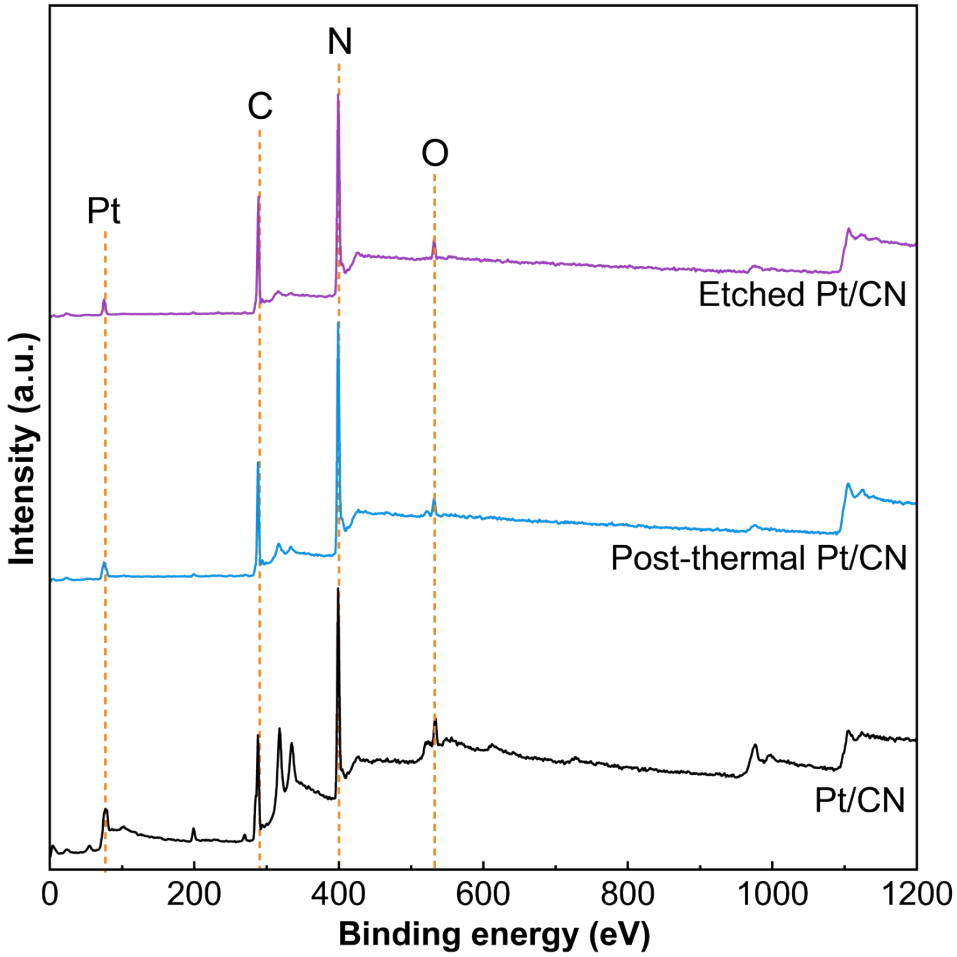

Figure S7. XPS survey spectra of CN. Wherein bulk Pt/CN (black), post-thermal Pt/CN (blue), and etched Pt/CN (purple).

An adventitious carbon peak located at 284.4 eV, designated as C 1s, was used to calibrate the binding energy. All of the spectra showed strong peaks at around 76.0 eV, 288.0 eV, 399.0 eV, and 533.0 eV, which correlated to Pt 4f, C 1s, N 1s, and O 1s, respectively. The small peaks at around 200 and 270 eV are ascribed to Cl 2p and Cl 2s respectively, which is remained from platinum precursor H_2PtCl_6.[1] The peak intensity of Cl 2p in bulk Pt/CN is higher than post-thermal and etched Pt/CN treatments. The peaks related to O and N KLL Auger are visible around 974 eV and 1105 eV BE, respectively.

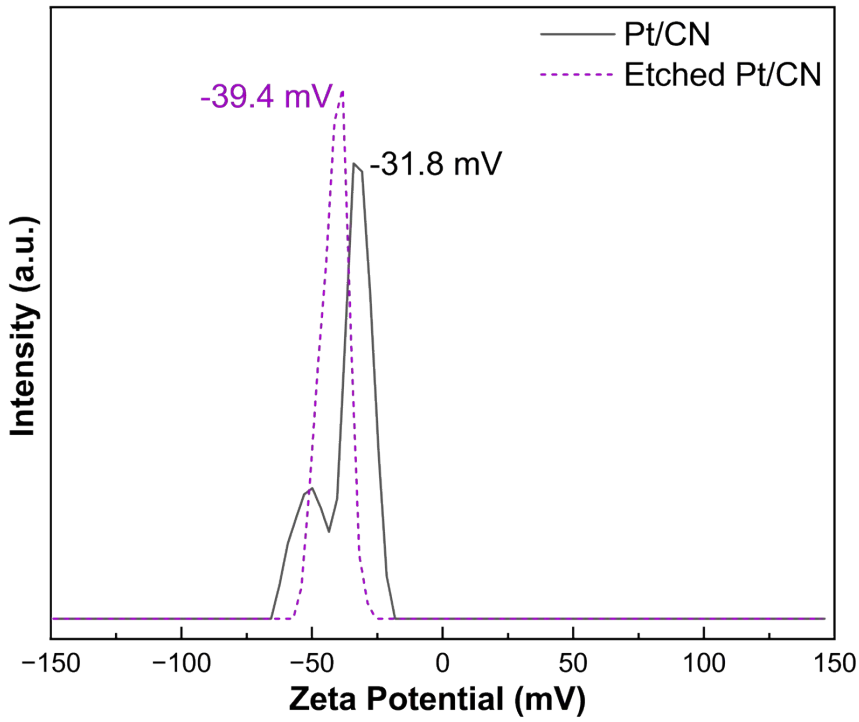

Figure S8. Zeta Potentials of bulk Pt/CN and etched Pt/CN samples at pH = 7. The bulk Pt/CN has a zeta potential of -31.4 mV, whereas the etched Pt/CN exhibits a greater negative zeta potential of -39.4 mV The increased zeta potential value indicates more surface groups for the etched Pt/CN as compared to the bulk CN sample.

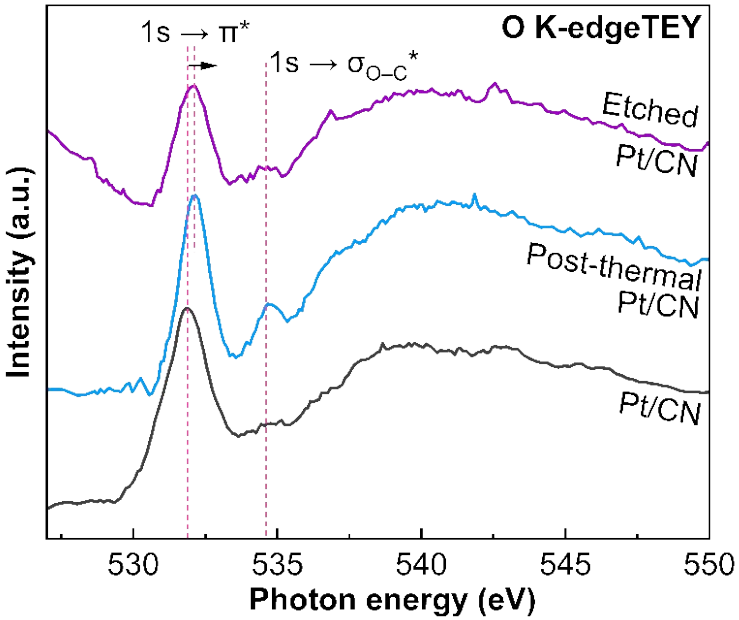

Figure S9. XAS spectra of O K-edge of bulk Pt/CN (black), post-thermal Pt/CN (blue), and etched Pt/CN (purple) acquired in Total Electron Yield (TEY) mode.

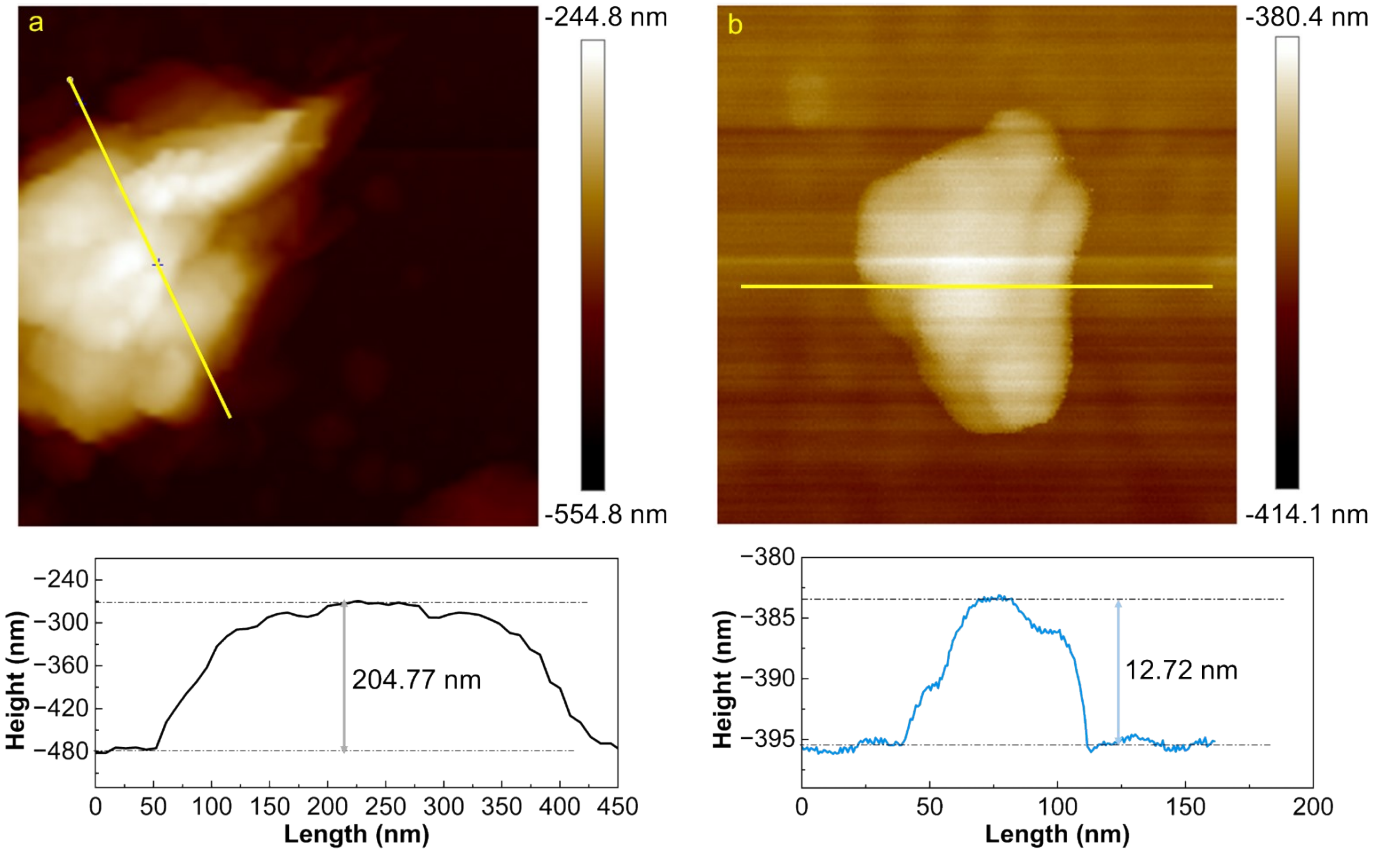

Figure S10. AFM image and height cutaway view of CN and post-thermal CN

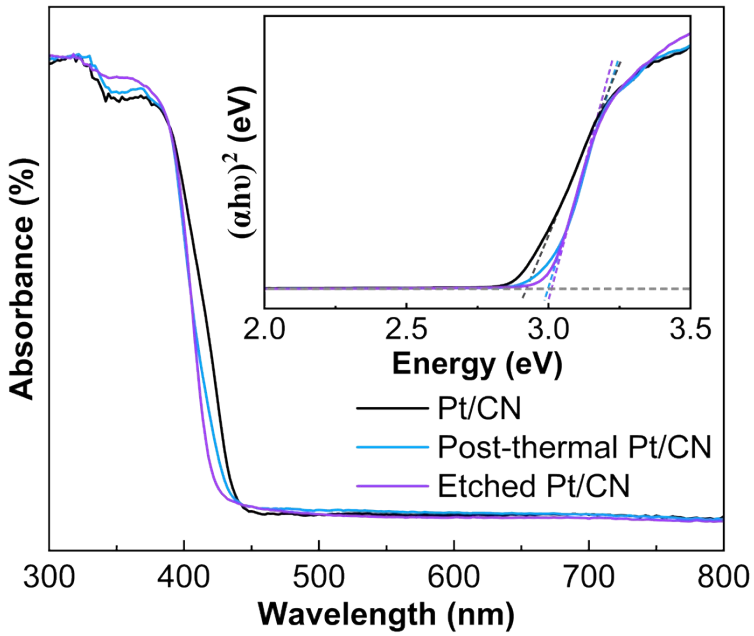

Figure S11. UV-vis diffuse reflectance spectra of CN. The spectra reveal broad absorption bands below 425 nm, along with a noticeable long-tail absorption extending from 425 to 455 nm. The optical bandgap was estimated from the intersection point between the long-tail and the primary absorption edge at 425 nm, yielding an approximate value of 3 eV, as shown in **Table 2** in main manuscript. Furthermore, Tauc's equation was employed to calculate the bandgap transition energy (E_g). Typically, the quantum confinement effect leads to an increase in the bandgap as the material's thickness decreases.[2]

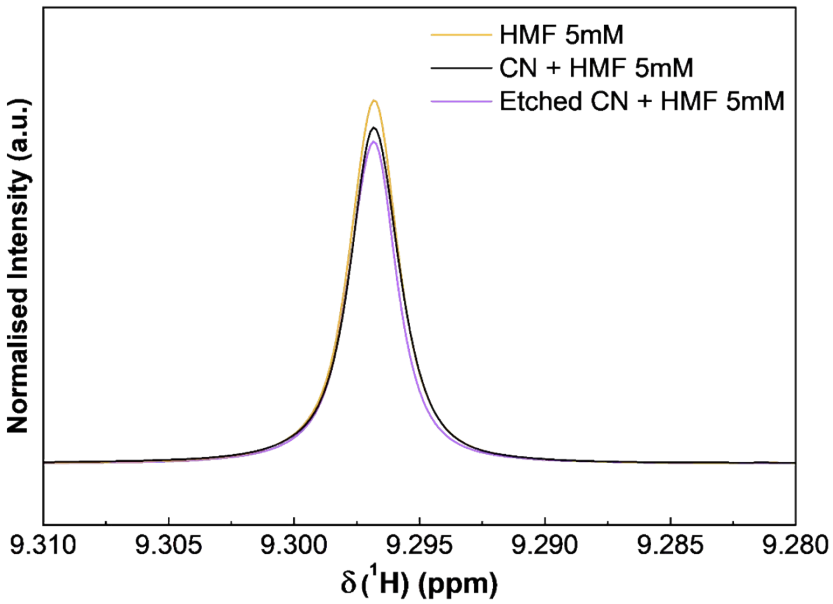

Figure S12. Enlarged spectral region (chemical shift range of 9.28-9.31 ppm) of 1D ^{1}H NMR spectra from HMF 5mM adsorption test with CN and etched CN.

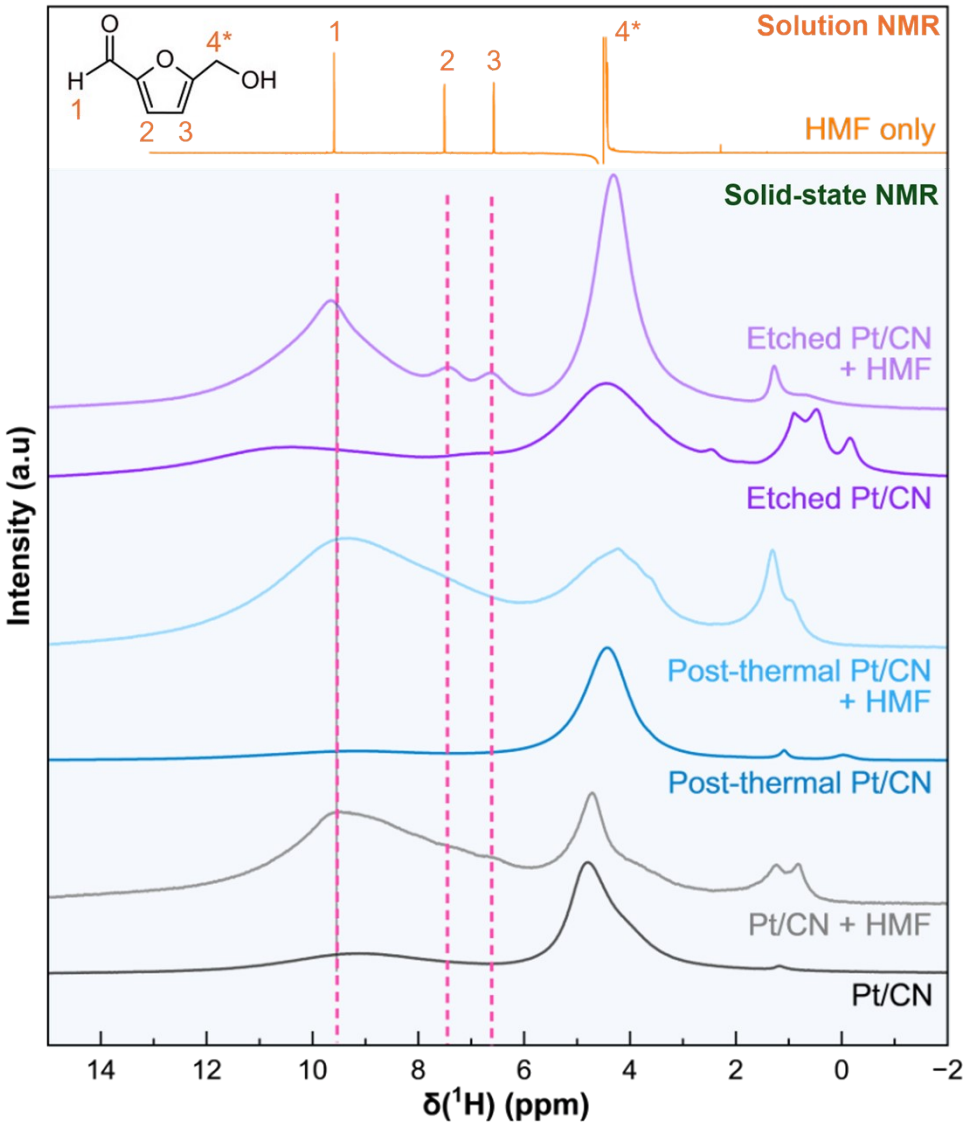

Figure S13. 1D ^{1}H NMR solid-state NMR spectra of photocatalyst with and without HMF adsorption. The furan signals are significantly stronger in the etched Pt/CN catalyst compared to the other two catalysts. 1H chemical shifts of these signals closely match those observed in 1D 1H solution NMR (orange in upper panel), confirming the presence of HMF in the solid sample. The other two HMF signals, corresponding to the -CH moiety and the aldehyde (-CHO) proton, are most likely obscured by the water peak and the broad downfield signal. Since the catalyst samples were insoluble in water and could not be analysed by solution NMR, the spectra were recorded using solid-state NMR.

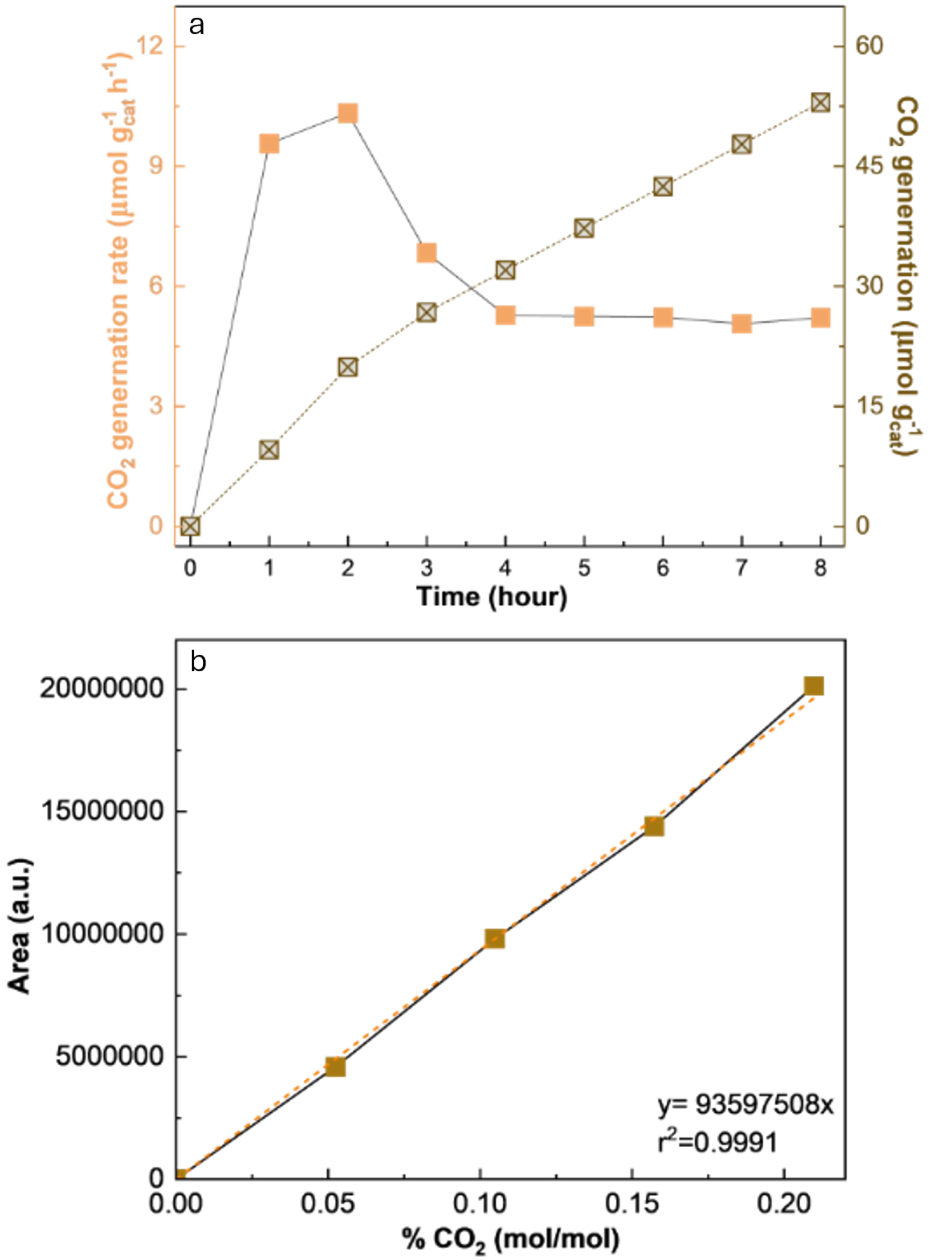

Figure S14. (a) CO_2 generation during HMF photoreforming over 8 hours. Experiment was conducted under simulated solar light conditions (AM 1.5G, 100 mW cm^{-2}, 23 ± 2 °C) utilising 100 mg of etched CN samples, with 3 wt% of Pt, reaction medium 100 ml HMF 5 mM under Ar-saturated atmosphere, (b) CO_2 calibration line obtained from GC-FID by diluting a standard gas mixture containing 0.2098 % (mol/mol) CO_2 (sourced from Coregas Australia Supplier) with Ar.

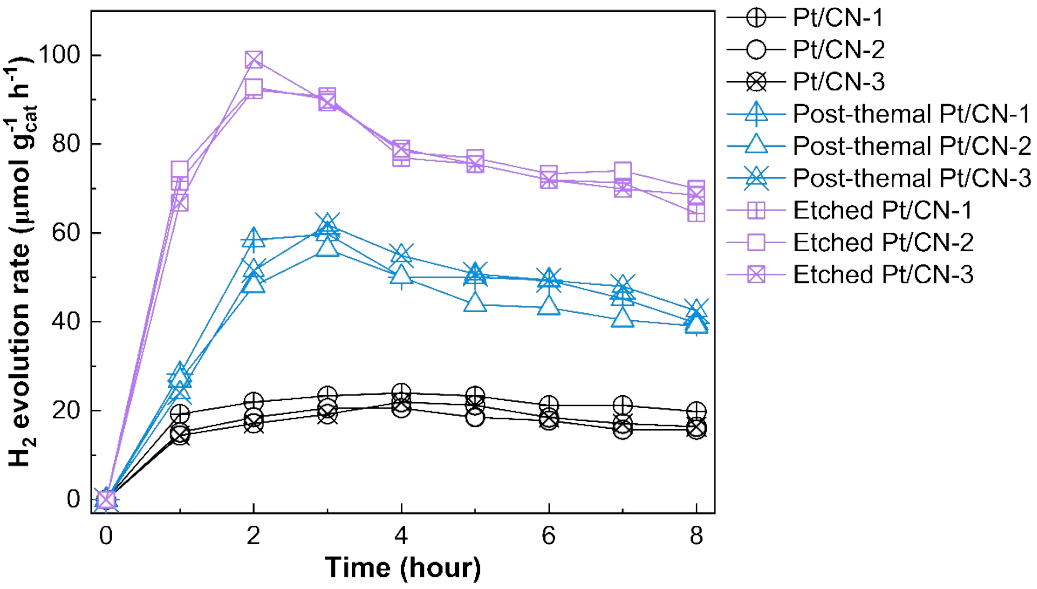

Figure S15. Hydrogen evolution performance was collected in 8 hours of photoreaction with Pt/CN (black), post-thermal Pt/CN (blue) and etched Pt/CN (purple). All experiments were conducted under simulated solar light conditions (AM 1.5G, 100 mW cm^{-2}, 23 ± 2 °C) utilising 100 mg of freshly CN samples, with 3 wt% of Pt, reaction medium 100 ml HMF 5 mM under Ar-saturated atmosphere

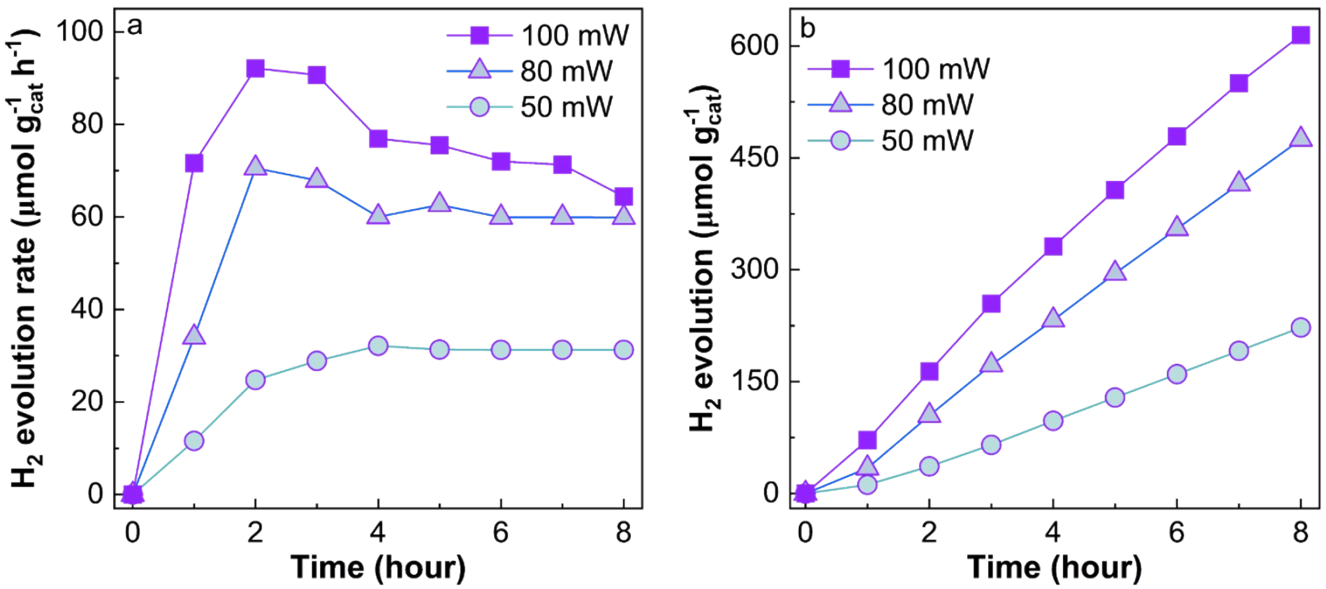

Figure S16. Hydrogen evolution performance was collected in 8 hours of photoreaction with etched Pt/CN using different light intensity. All experiments were conducted under simulated solar light conditions (AM 1.5G, 100 mW cm^{-2}, 23 ± 2 °C) utilising 100 mg of etched CN samples, with 3 wt% of Pt, reaction medium 100 ml HMF 5 mM under Ar-saturated atmosphere.

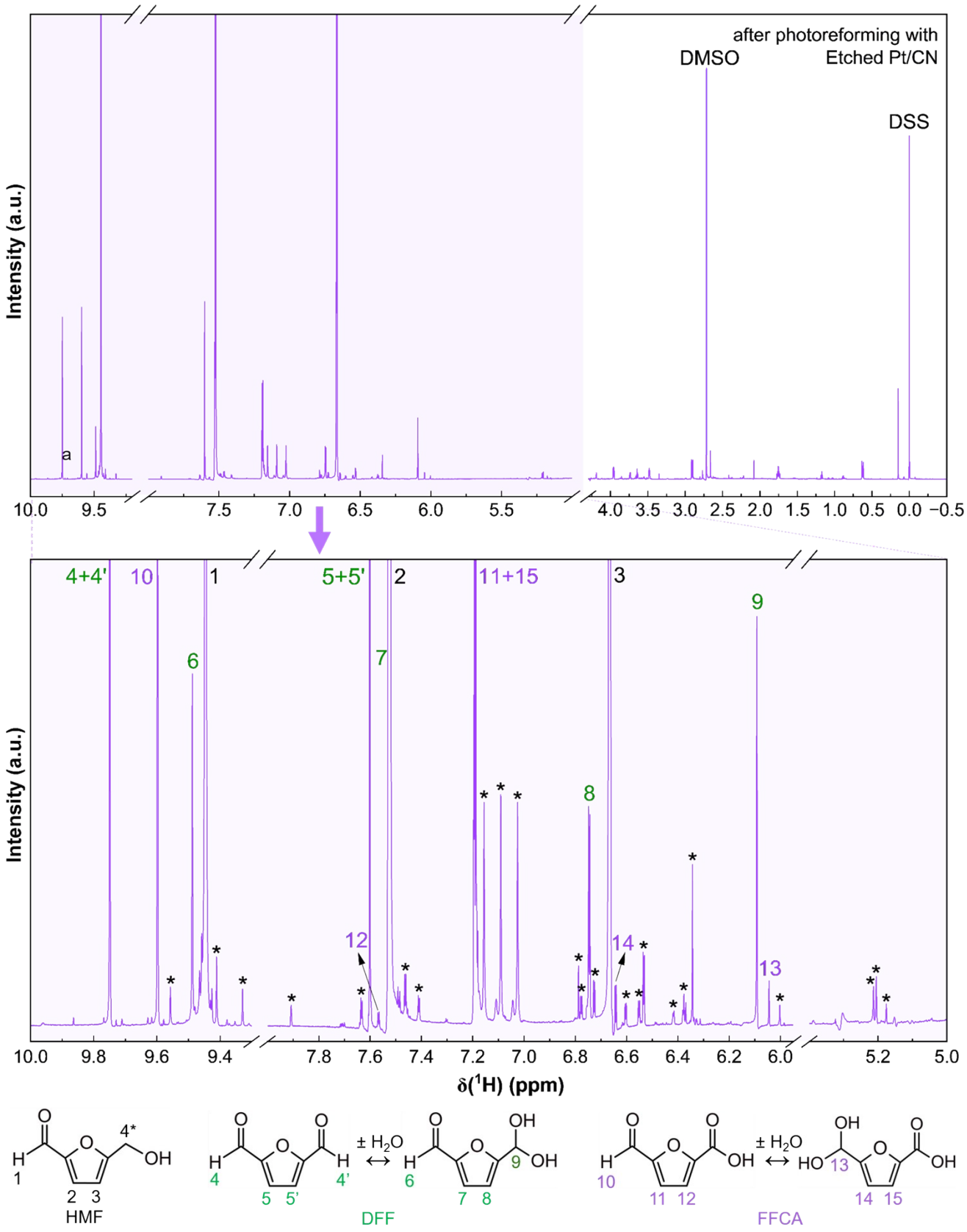

Figure S17. Upper panel: 1D ^{1}H NMR of HMF after photoreforming with etched Pt/CN. Lower panel: Enlarged spectral region (chemical shift range of 5-10 ppm) of HMF after photoreforming with etched Pt/CN, showing the distinct separation of HMF, DFF and FFCA signals. Asterisk (∗) correspond to unassigned signals.

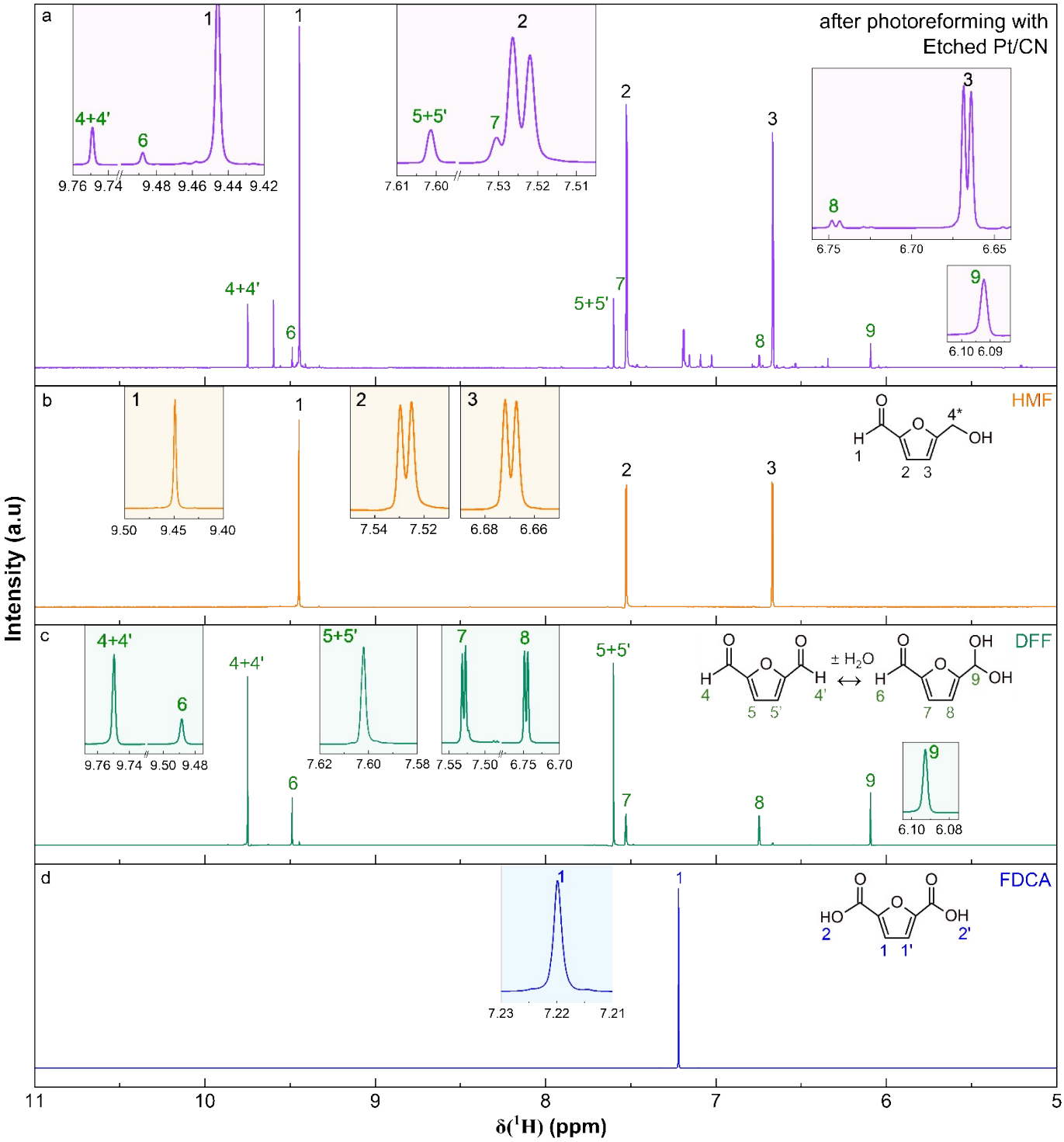

Figure S18. Detail peaks position of 1D ^{1}H NMR of (a) HMF after photoreforming with etched Pt/CN, highlighting the key signals of HMF and DFF. (b-d) Spiked 1D ^{1}H NMR spectra of HMF, DFF, FCDA are shown as reference, which allowed to verify the ^{1}H chemical shift assignments of NMR signals observed from HMF sample after photoreforming with etched Pt/CN. All samples were prepared in identical NMR buffer. DSS and DMSO signals region was removed for clarity.

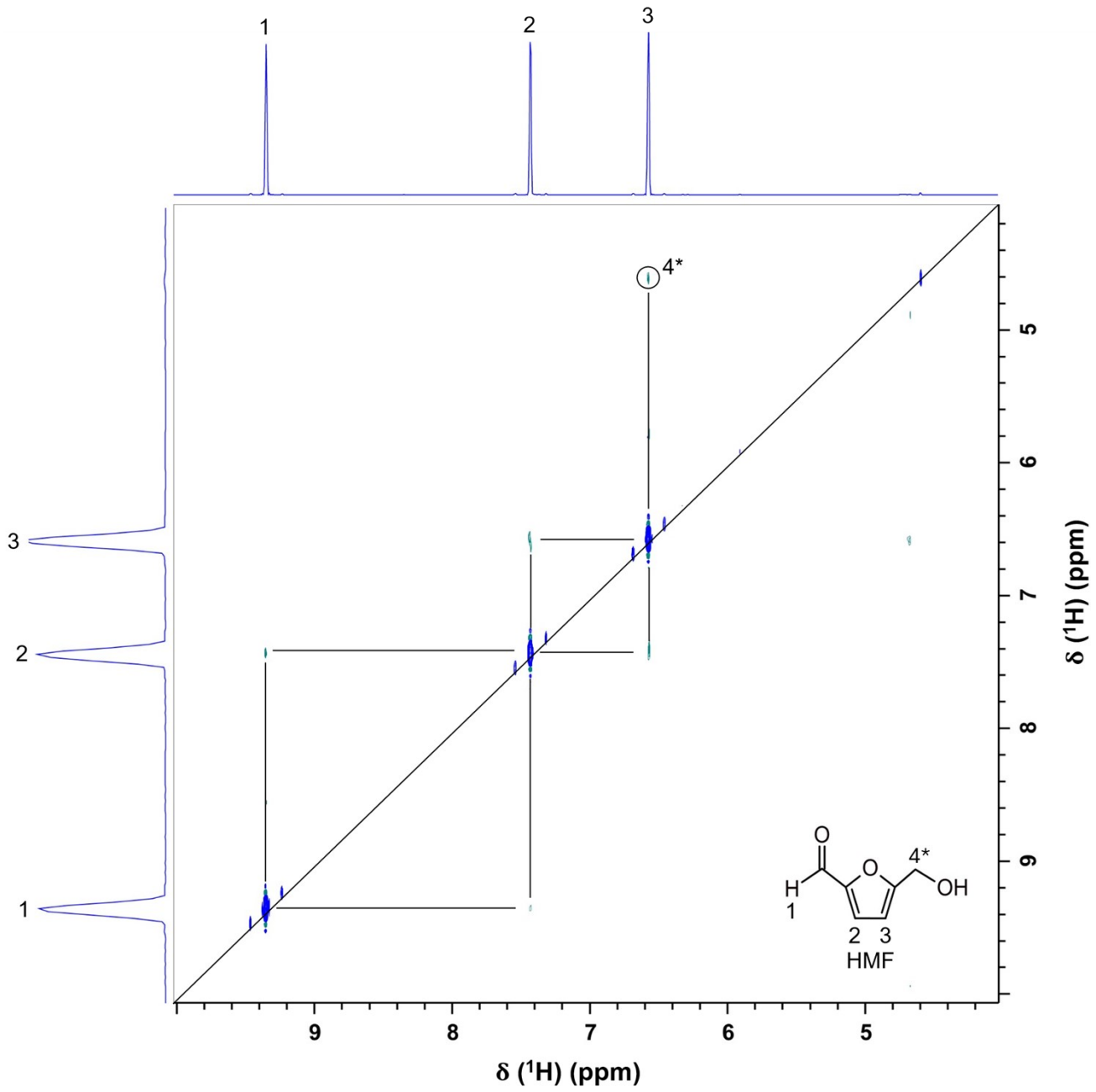

Figure S19. 2D [^{1}H,^{1}H]-NOESY spectrum of 5 mM HMF in 95% (v/v) H_2O, 5% (v/v) D_2O, 0.1 mM DMSO, and 0.1 mM DSS. The spectrum was collected on an 800 MHz spectrometer at 25 °C. The ^{1}H chemical shift of the two benzylic protons (labelled as 4* in the structure) of HMF is at 4.6 ppm, which is close to the water signal and likely suppressed by the water suppression pulse sequence used during ^{1}D 1H NMR data collection. However, NOE cross peak (green) between the benzylic protons and the furan ring proton (labelled as 3 in the structure) was distinctly observed in the NOESY, indicating their proximity. The NOE mixing time of 800 ms was used to collect the NOESY data.

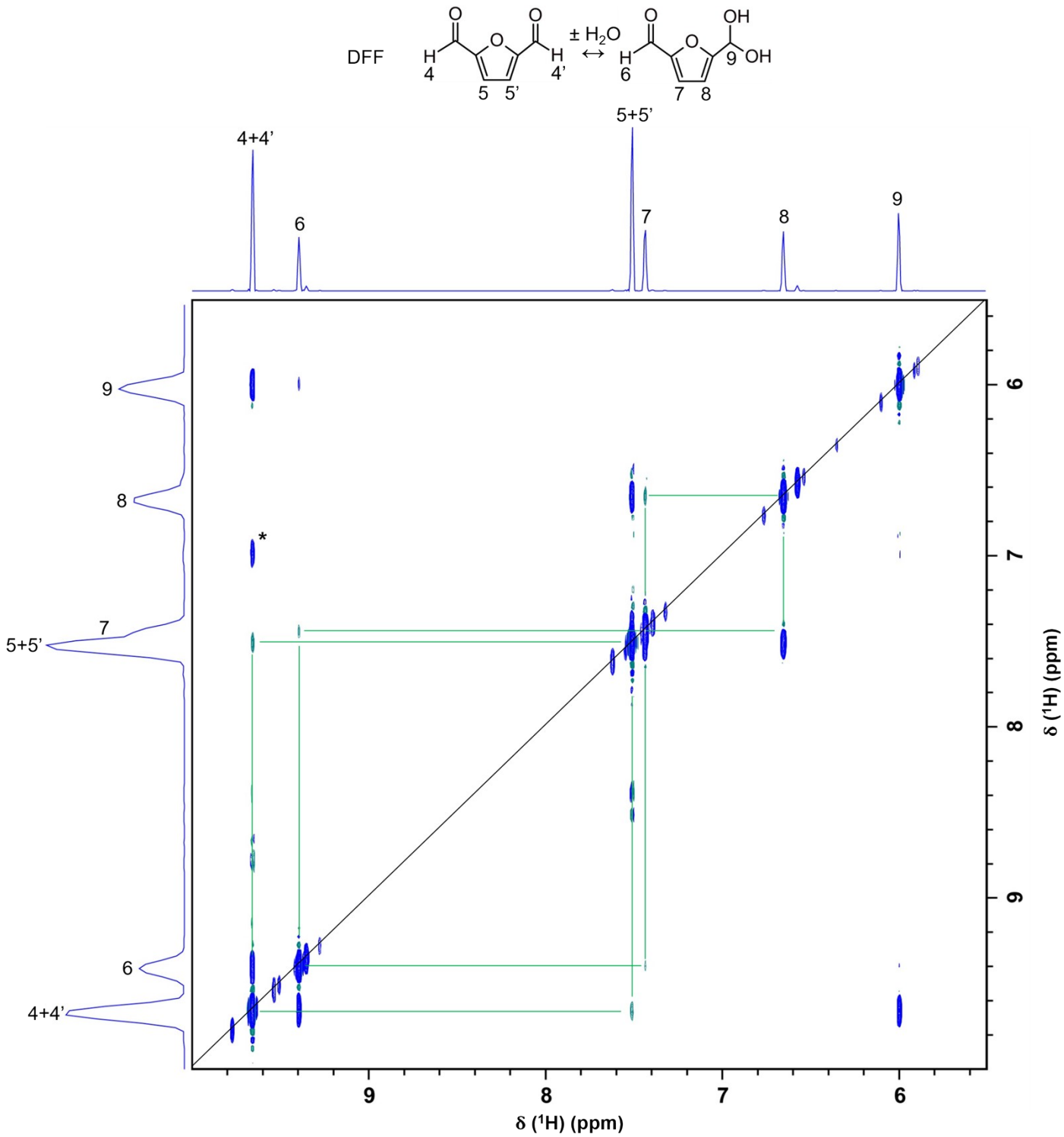

Figure S20. 2D [^{1}H,^{1}H]-NOESY NMR spectrum of 5 mM DFF in aqueous NMR buffer (95% (v/v) H_2O, 5% (v/v) D_2O, 0.1 mM DMSO, and 0.1 mM DSS), which shows a set of NOE cross peaks in same and other sets in opposite phase of diagonal peaks, indicating intramolecular cross peaks (green) and chemical exchange cross peaks (blue) of hydrated and unhydrated form of DFF in aqueous solvent. The cross peak at 6.98 ppm (labelled as asterisk) doesn't have a symmetric peak across the diagonal, so likely an artefact peak. To distinguish the intramolecular NOE cross peaks from chemical exchange peaks, the intramolecular cross peaks are indicated with dotted green lines. The NOE mixing time of 600 ms was used to collect the NOESY data.

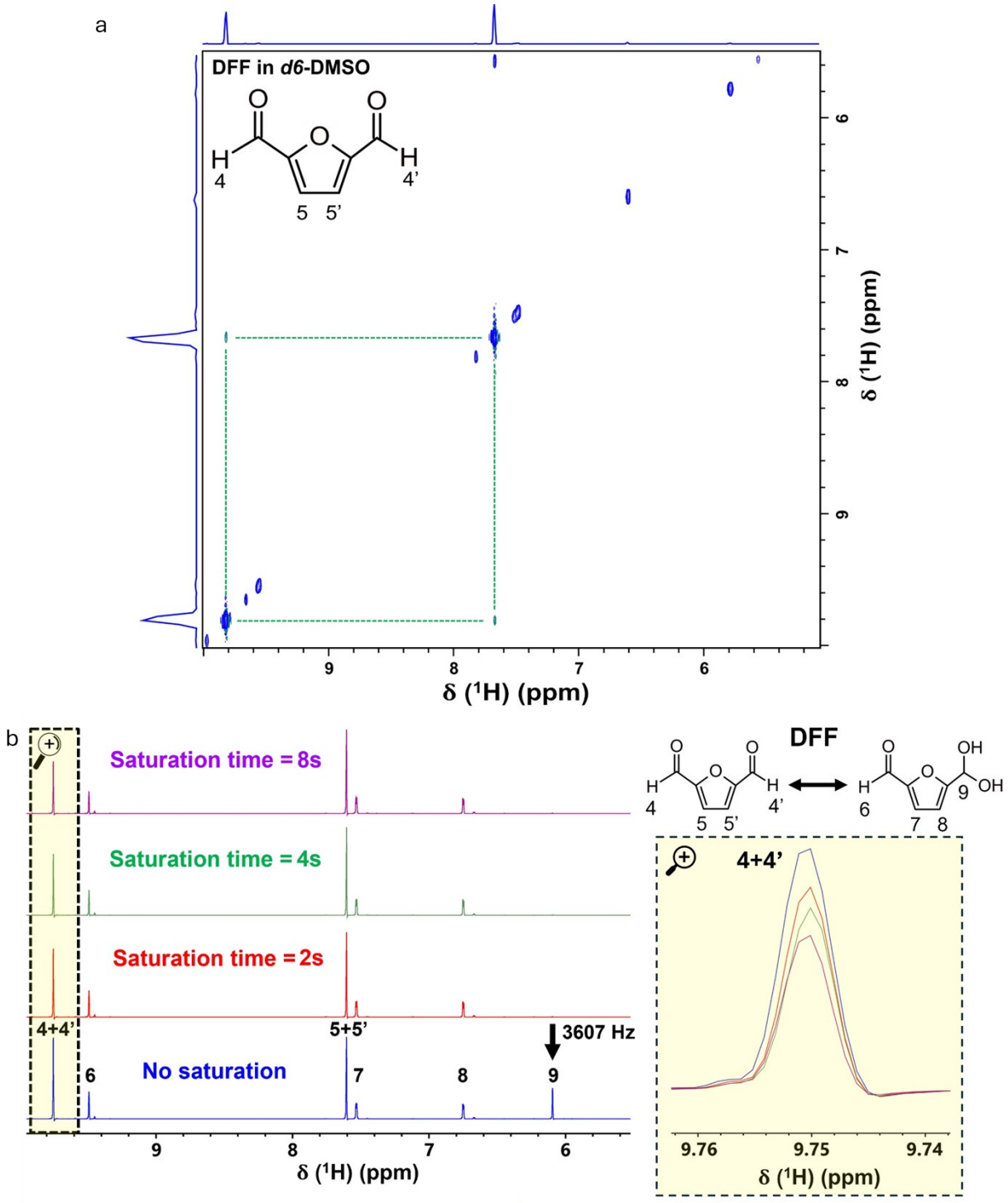

Figure S21. (a) 2D [^{1}H,^{1}H]-NOESY spectrum of DFF in d_6-DMSO, acquired with a 600 ms NOE mixing time on a 600 MHz spectrometer equipped with a Z-gradient CryoProbe at 25 °C. As expected, only intramolecular NOE cross-peaks (highlighted in green) were observed, consistent with the close spatial proximity of the two protons within the DFF molecule. (b) 1D ^{1}H NMR spectra of DFF with and without selective saturation at 6.1 ppm, collected on a 600 MHz spectrometer equipped with a Z-gradient CryoProbe at 25 °C at varying saturation times. Selective saturation of the isolated peak at 3607 Hz (labelled as 9) resulted in a clear decrease in the signal at 9.75 ppm (labelled as 4+4', its enlarged region is shown in the upper right), indicating chemical exchange between the hydrated and unhydrated forms of DFF in aqueous solution.

Table S2. The apparent energy consumption to produce H_2, DFF and FFCA.

Product	**Amount produced in 24 hours (mmol)**	**Energy input (kWh)**	**Apparent energy consumption (AEC, kWh mol^{-1})**
H_2	0.1247	0.0672	~538.9
DFF	0.0386	0.0672	~1740.9
FFCA	0.0292	0.0672	~2301.4

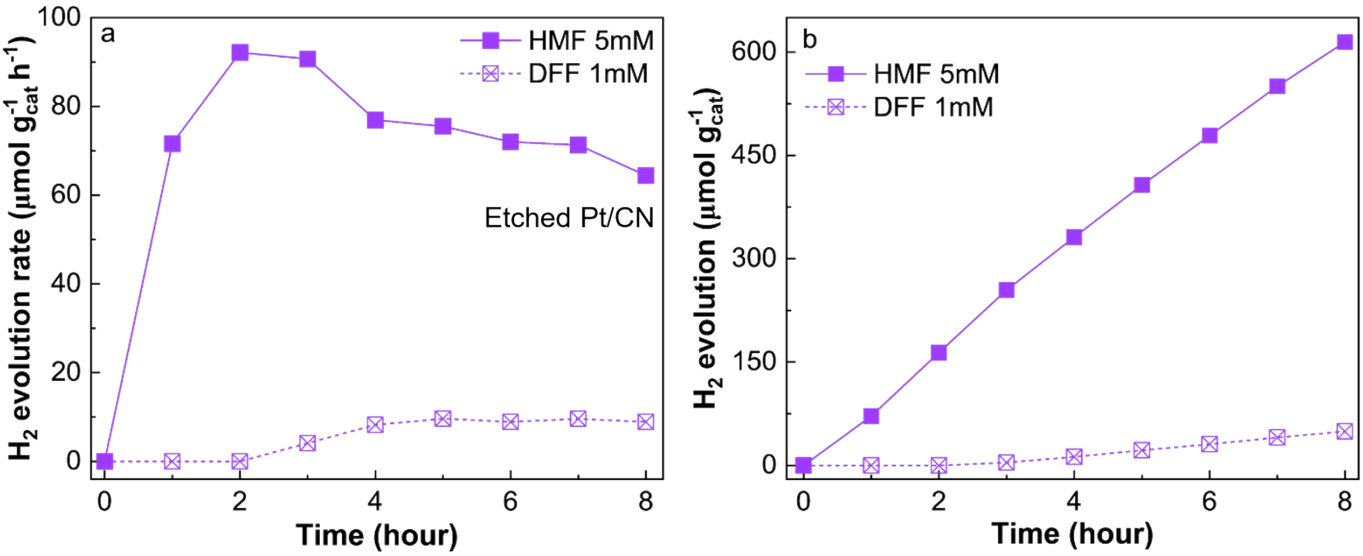

Figure S22. Hydrogen evolution performance was collected in 8 hours of photoreaction with etched Pt/CN using HMF and DFF as sacrificial agents. All experiments were conducted under simulated solar light conditions (AM 1.5G, 100 mW cm^{-2}, 23 ± 2 °C) utilising 100 mg of etched CN samples, with 3 wt% of Pt, reaction medium 100 ml HMF 5 mM under Ar-saturated atmosphere.

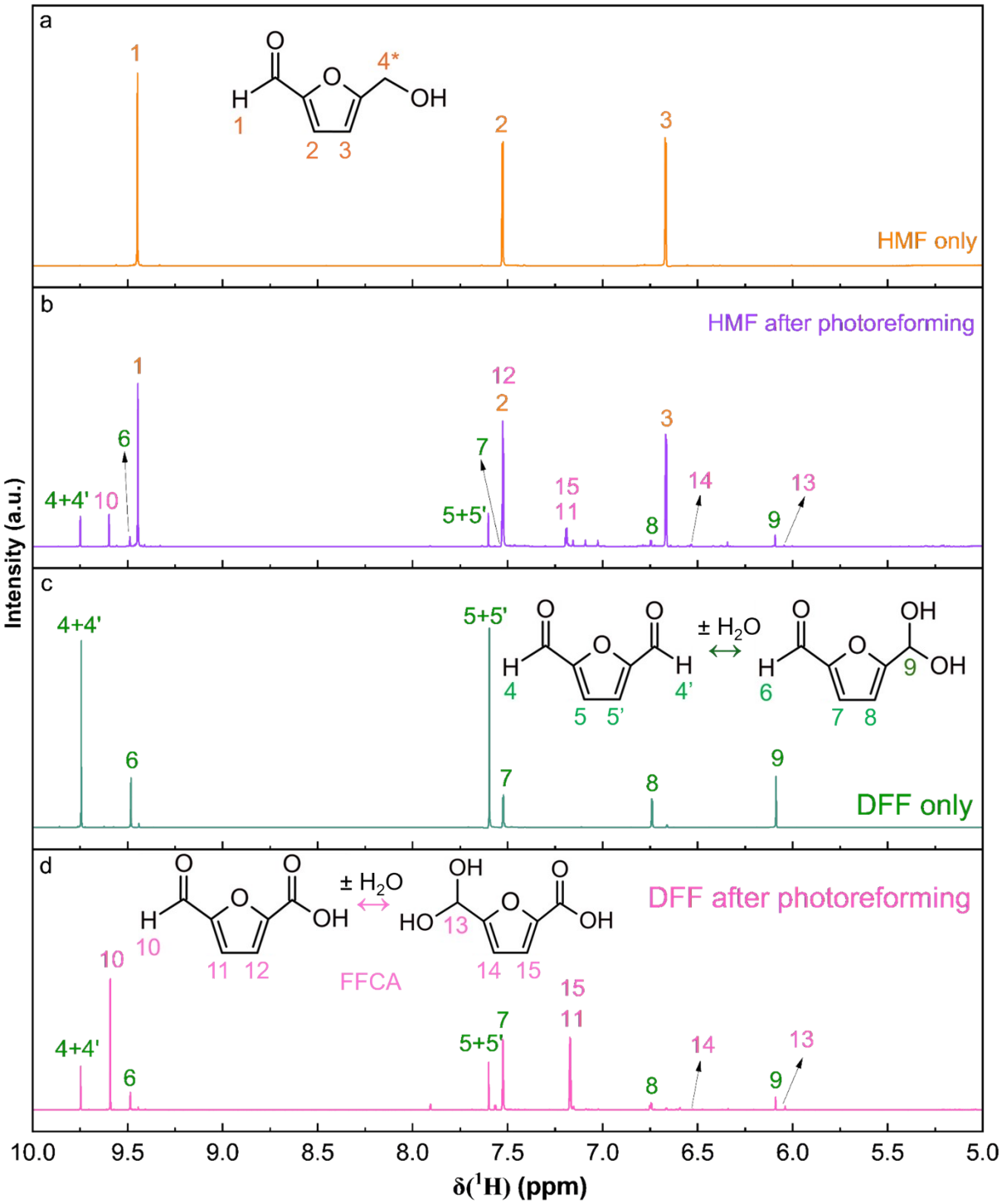

Figure S23. 1D ^{1}H NMR spectra from HMF after photoreforming in 24 hours and DFF after photoreforming in 12 hours over etched Pt/CN. All experiments were conducted under simulated solar light conditions (AM 1.5G, 100 mW cm^{-2}, 23 ± 2 °C) utilising 100 mg of etched CN samples, with 3 wt% of Pt, reaction medium 100 ml HMF 5 mM or 100 ml DFF 1 mM under Ar-saturated atmosphere.

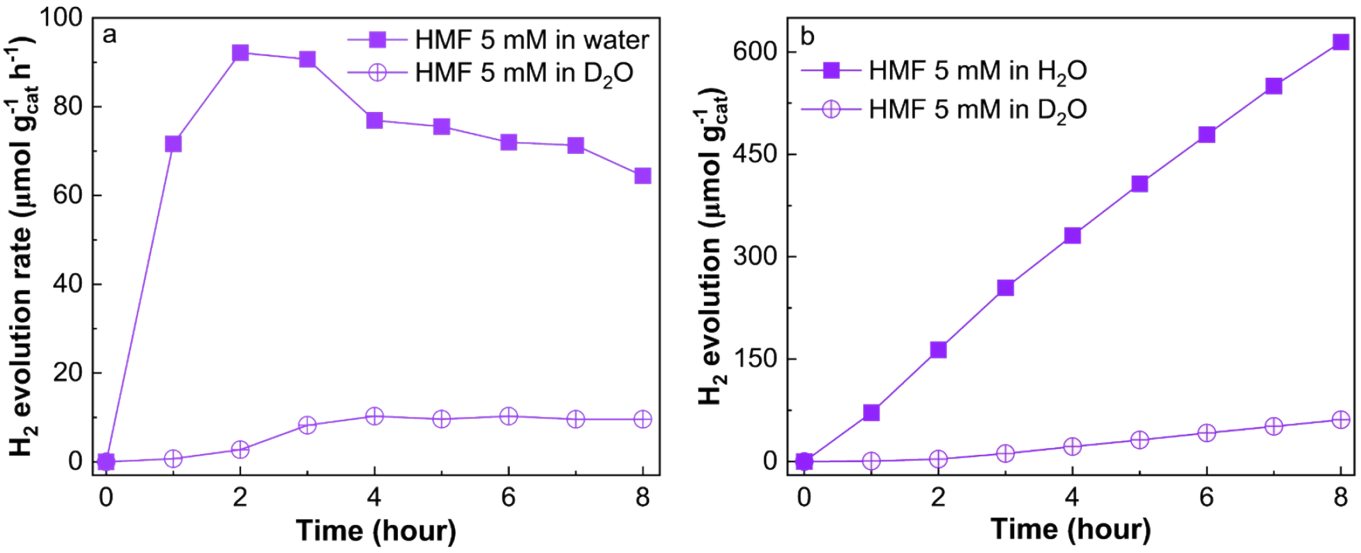

Figure S24. Hydrogen evolution performance was collected in 8 hours HMF photoreforming with etched Pt/CN in D_2O and H_2O. All experiments were conducted under simulated solar light conditions (AM 1.5G, 100 mW cm^{-2}, 23 ± 2 °C) utilising 100 mg of etched CN samples, with 3 wt% of Pt, reaction medium 100 ml HMF 5 mM under Ar-saturated atmosphere.

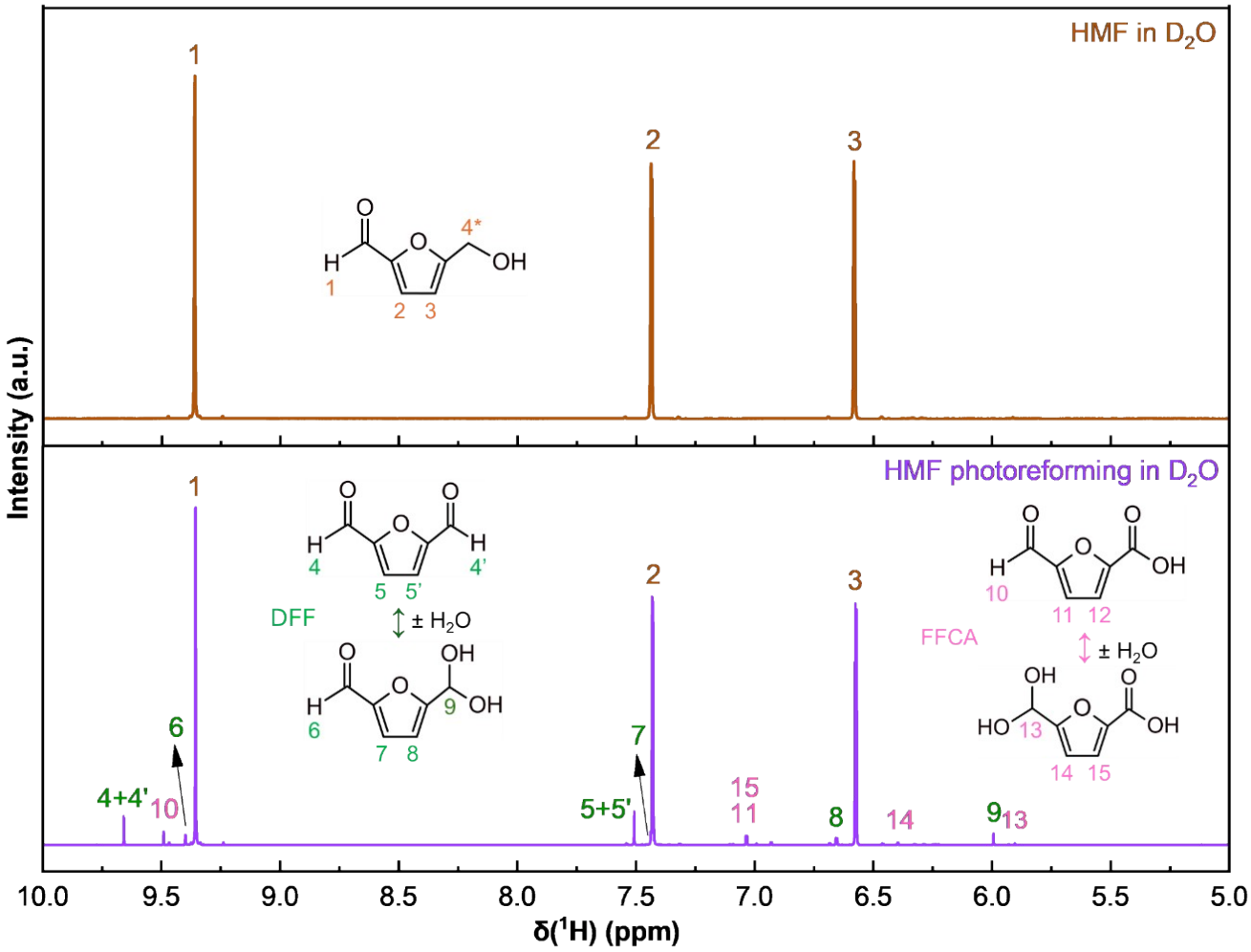

Figure S25. 1D ^{1}H NMR spectra from HMF after photoreforming in D_2O over 8 hours using etched Pt/CN. All experiments were conducted under simulated solar light conditions (AM 1.5G, 100 mW cm^{-2}, 23 ± 2 °C) utilising 100 mg of etched CN samples, with 3 wt% of Pt, reaction medium 100 ml HMF 5 mM or 100 ml DFF 1 mM under Ar-saturated atmosphere.

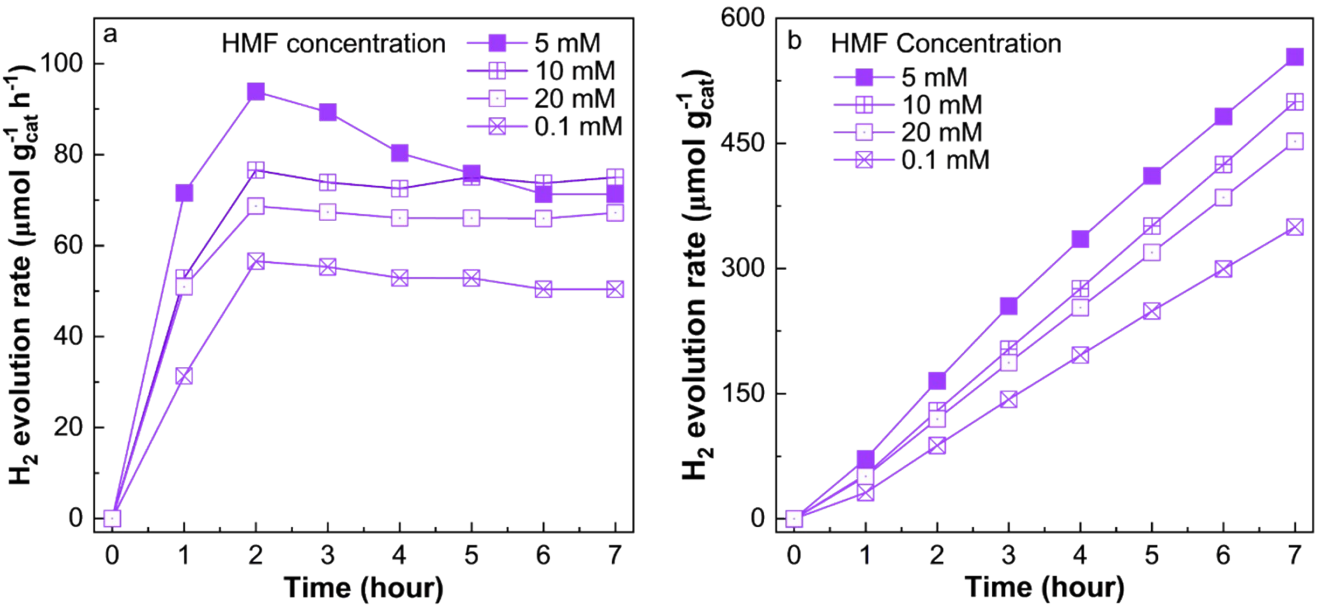

Figure S26. (a) H_2 evolution rate and (b) accumulated H_2 over 7 h of photoreaction using etched Pt/CN with varying HMF concentrations. All experiments were conducted under simulated solar light conditions (AM 1.5G, 100 mW cm^{-2}, 23 ± 2 °C) utilising 100 mg of etched CN samples, with 3 wt% of Pt, reaction medium 100 ml HMF 5 mM under Ar-saturated atmosphere.

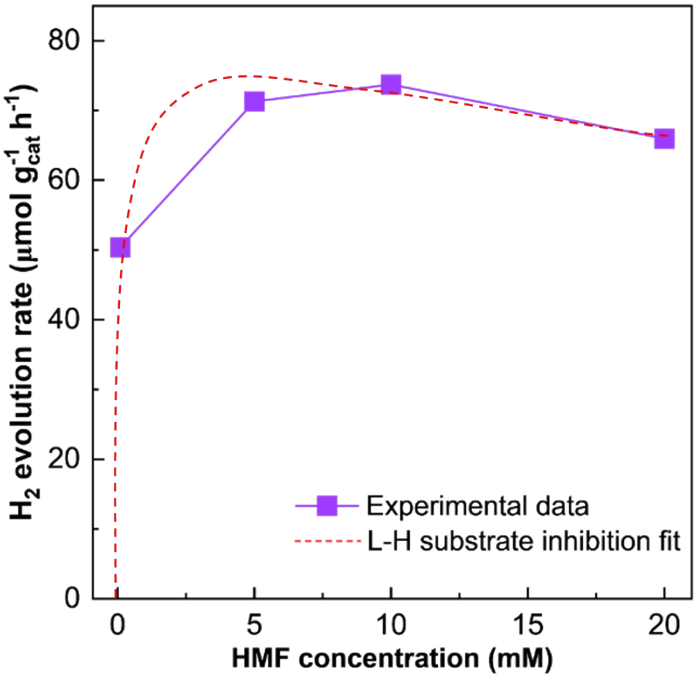

Figure S27. Plot showing H_2 evolution rates at 6th hour of reaction versus HMF concentration. The purple points are the experimental H_2 evolution rates data, and the red curve is fitted Langmuir-Hinshelwood model. All experiments were conducted under simulated solar light conditions (AM 1.5G, 100 mW cm^{-2}, 23 ± 2 °C) utilising 100 mg of etched CN samples, with 3 wt% of Pt, reaction medium 100 ml HMF 5 mM under Ar-saturated atmosphere.

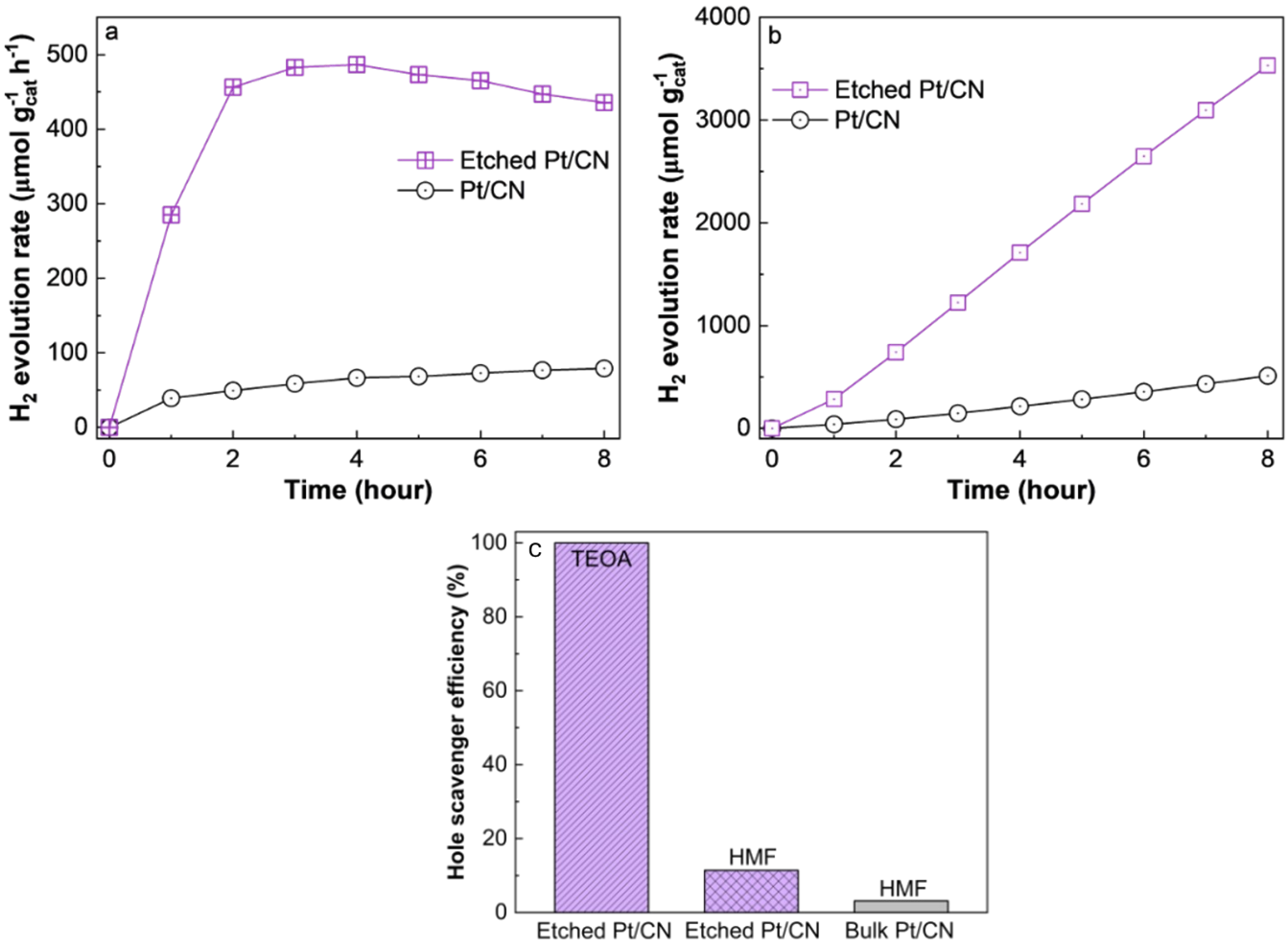

Figure S28. (a) hydrogen evolution rate and (b) the corresponding overall hydrogen yield using bulk Pt/CN (empty-black circle) and etched Pt/CN (empty-square purple) using TEOA as sacrificial agent. All experiments were conducted under simulated solar light conditions (AM 1.5G, 100 mW cm^{-2}, 23 ± 2 °C) utilizing 100 mg of freshly as-prepared CN, with 3 wt% of Pt, reaction medium 100 ml solution with 10 V% TEOA (10 ml TEOA) under Ar-saturated atmosphere.

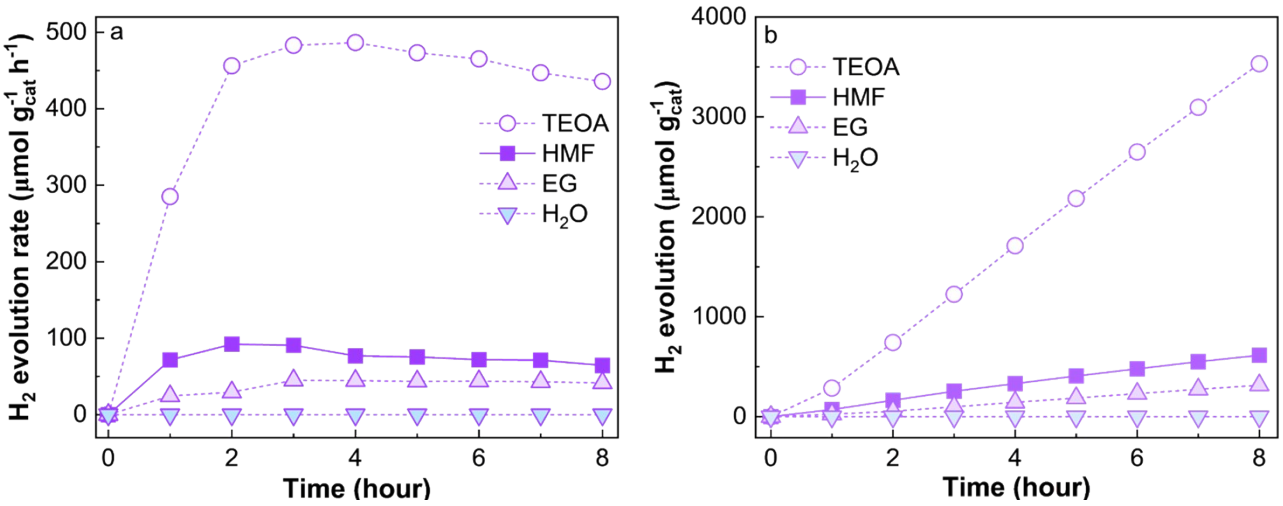

Figure S29. Hydrogen evolution rate when using different electron donors, including TEOA, HMF, EG, and pure water. All experiments were conducted under simulated solar light conditions (AM 1.5G, 100 mW cm^{-2}, 23 ± 2 °C) utilising 100 mg catalyst samples, with 3 wt% of Pt, reaction medium 100 ml HMF 5 mM under Ar-saturated atmosphere.

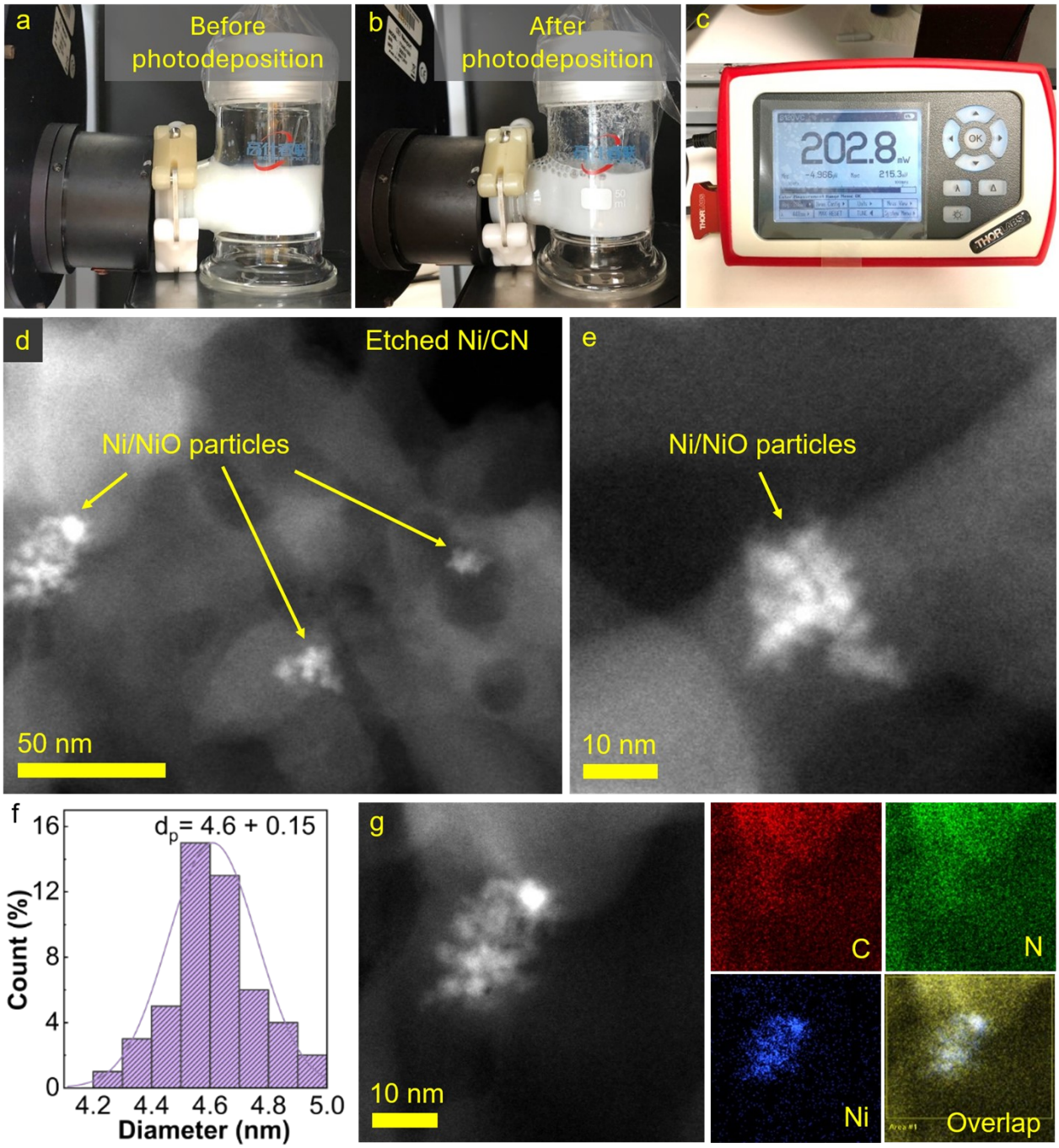

Figure S30. (a) Ni loading etched CN solution before photodeposition and (b) after photodeposition in 15 hours, (c) light intensity used for Ni photodeposition, (d) TEM, (e) HR-TEM images, (f) Ni/NiO size distribution and (g) EDX elemental mapping analysis of etched Ni/CN showing carbon (red), nitrogen (green), nickel (blue).

The HR-TEM images show Ni deposition with the agglomerated particle size around 4.6 ± 0.15 nm on etched Pt/CN. EDX mapping images shown the well distribution of Ni, as well as C and N atoms, prove the successful photodeposition of Ni particles.

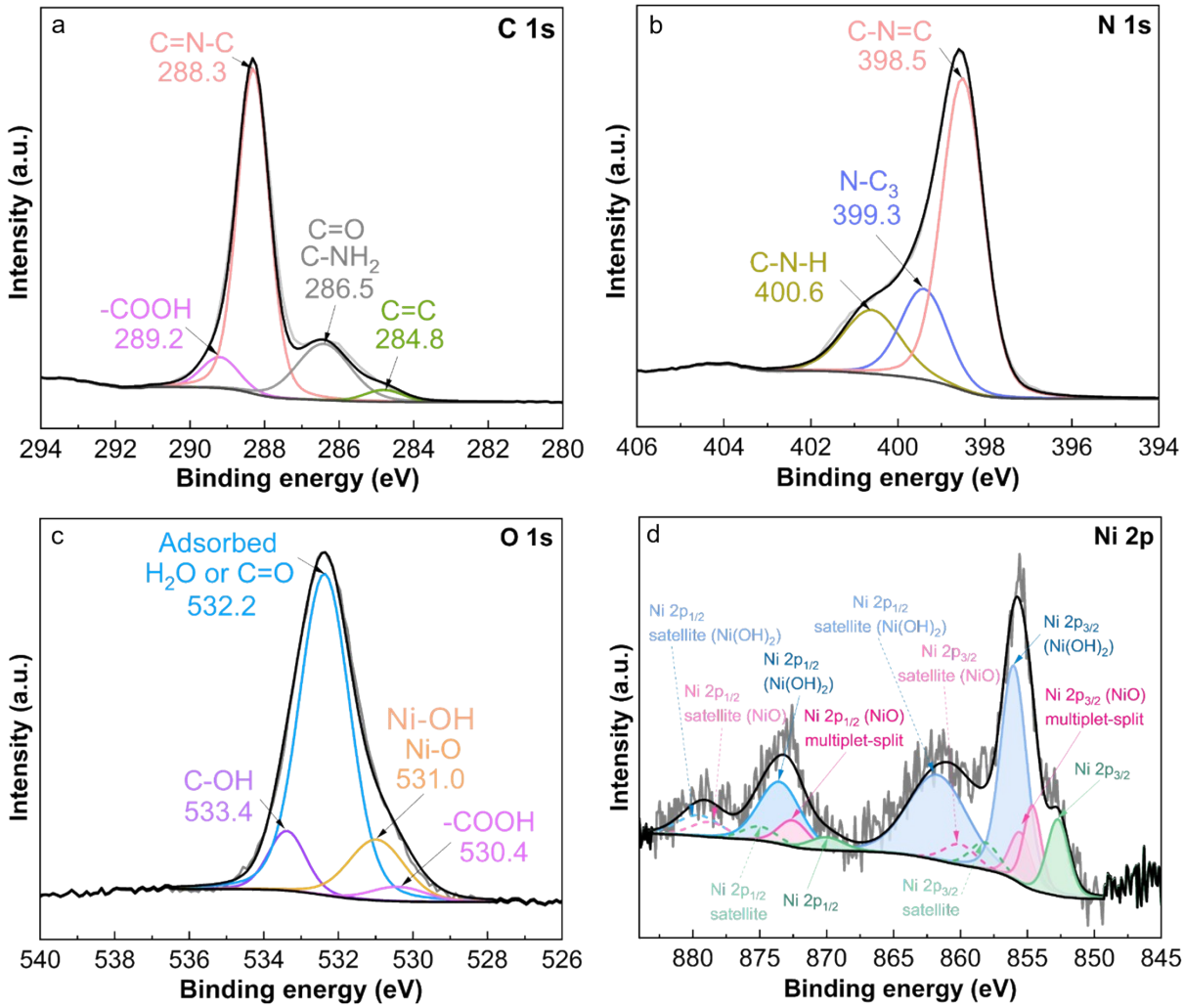

Figure S31. XPS spectra of (a) C 1s, (b) N 1s, (c) O 1s, (f) Ni 2p.

X-ray photoelectron spectroscopy (XPS) was performed to examine the chemical states and surface composition of the etched Ni/CN photocatalyst. The C 1s spectrum (**Figure S29a**) displays characteristic peaks at 284.8 eV (sp^2 C-C/C=C), 286.2 eV (C-NH_2/C=O), 288.3 eV (C-N=C), and 289.2 (-COOH) confirming the intact heptazine framework of CN with oxygen-functional groups via chemical oxidation. The N 1s spectrum (**Figure S29b**) can be deconvoluted into contributions at 398.5 eV (C=N-C, sp^2-hybridized N), 399.3 eV (N-$(C)_3$, tertiary nitrogen), and 400.6 eV (C-N-H), along with a minor shake-up feature at higher binding energy, consistent with the polymeric CN structure. The O 1s spectrum (**Figure S29c**) shows peaks around 530.4 eV (-COOH), 531.0 eV (Ni-O/Ni-OH), 532.2 eV (adsorbed oxygen species or C=O), and 533.4 (C-OH) suggesting surface functional groups and partial Ni-O/NiOH bonding. Importantly, the Ni 2p spectrum (**Figure R29d**) of the etched Ni/CN shows well-defined spin-orbit doublets and satellite features, confirming the coexistence of multiple nickel species.[3] The multiplet-split peaks at 852.7 eV (Ni $2p_{3/2}$) and 870 eV (Ni $2p_{1/2}$) are assigned to metallic Ni^0. Signals cantered at 855.5 and 854.6 eV (multiplet-split Ni $2p_{3/2}$) and 873 eV (Ni $2p_{1/2}$), accompanied by satellites, correspond to Ni^{2+} in NiO. Additionally, the peaks at 856 eV (Ni $2p_{3/2}$) and 873.5 eV (Ni $2p_{1/2}$) can be attributed to Ni^{2+} in $Ni(OH)_2$. The presence of both oxide and hydroxide species indicates surface oxidation/hydroxylation of Ni under the etching process, while the minor metallic Ni component suggests partial preservation of zero-valent Ni. This combination implies that Ni exists in a mixed state, with oxidized species dominating the surface environment.

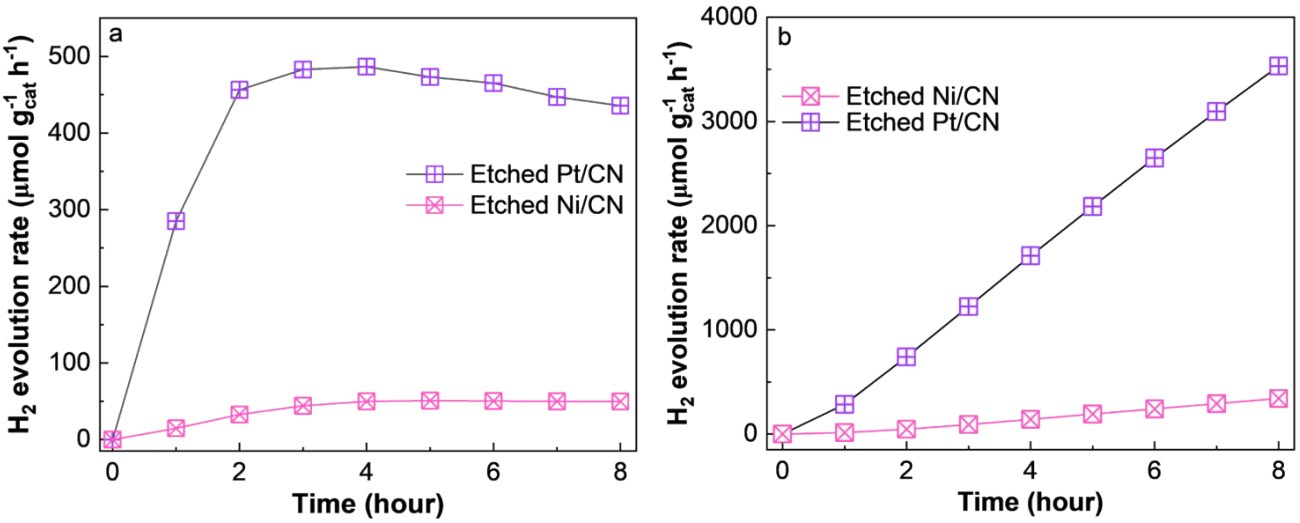

Figure S32. Hydrogen evolution performance was collected in 8 hours of photoreaction with etched Pt/CN using platinum and nickel as co-catalyst. All experiments were conducted under simulated solar light conditions (AM 1.5G, 100 mW cm^{-2}, 23 ± 2 °C) utilising 100 mg of etched CN samples, with 3 wt% of Pt, reaction medium TEOA 10 vol% in aqueous solution under Ar-saturated atmosphere.

Table S3. Pt concentration remaining in solution after HMF photoreforming.

Samples	Pt wt % after 8 h	Pt wt % after 24 h	Pt wt % after 2 days	Pt wt % after 3 days	Pt wt % after 5 days
	Unwashed catalyst after Pt photodeposition		Catalyst was washed after Pt photodeposition		
Pt/CN	0.35	0.26	-	-	-
Post-thermal Pt/CN	0.38	0.17	-	-	-
Etched Pt/ECN	0.25	0.14	LoD	LoD	LoD

LoD: Low of detection.

Table S4. Common solvents in HMF production and potential residues.

Potential solvent	Function in HMF Production	Boiling Point (°C)	Possible Residual Level (Typical Range)*	Notes	Ref
Water (H_2O)	Reaction medium (especially in acid-catalysed dehydration)	100	<0.5–2 wt%	Easily removed by drying or distillation	[4]
Dimethyl sulfoxide (DMSO)	High-yield polar solvent; stabilizes intermediates	189	0.1–10 wt%	Hard to remove; high boiling point; may interfere with catalysis	[5–7]
γ-Valerolactone (GVL)	Green solvent; used in biomass conversion	207	0.1–5 wt%	Biodegradable; can be partially removed by solvent extraction	[8]
Methyl isobutyl ketone (MIBK)	Extractant in biphasic systems (e.g., H_2O/MIBK)	116	<0.1–0.5 wt%	Often efficiently separated; toxic in high amounts	[4]
Acetonitrile (MeCN)	Co-solvent in some catalytic systems	82	<0.1 wt% (volatile)	Low boiling point; easy to remove	[9]
Dimethylformamide (DMF)	Polar solvent for sugar dissolution	153	0.1–3 wt%	Toxic; requires extensive removal	[10]
1,4-Dioxane	Solvent for high selectivity	101	<0.1–1 wt%	May form peroxides; moderately toxic	[11]
Tetrahydrofuran (THF)	Co-solvent; increases reaction rate	66	<0.1 wt%	Easily removed; flammable	[12]
Ethanol / Isopropanol	Green solvents; used for extractions or reaction medium	78 / 82	<0.1–0.5 wt%	Often co-evaporated with water	[13]

Ionic Liquids	Reaction media and catalysts (e.g., [EMIM][Cl])	>300	0.5–10 wt%	Very hard to remove; may contaminate HMF	[10]

* **Note**: Residual amounts are estimated ranges based on reported experimental results and purification strategies (e.g., solvent removal under vacuum, aqueous workup, or distillation). Trace levels (<0.1 wt%) are typically achievable with intensive purification, while crude HMF may contain significantly more.

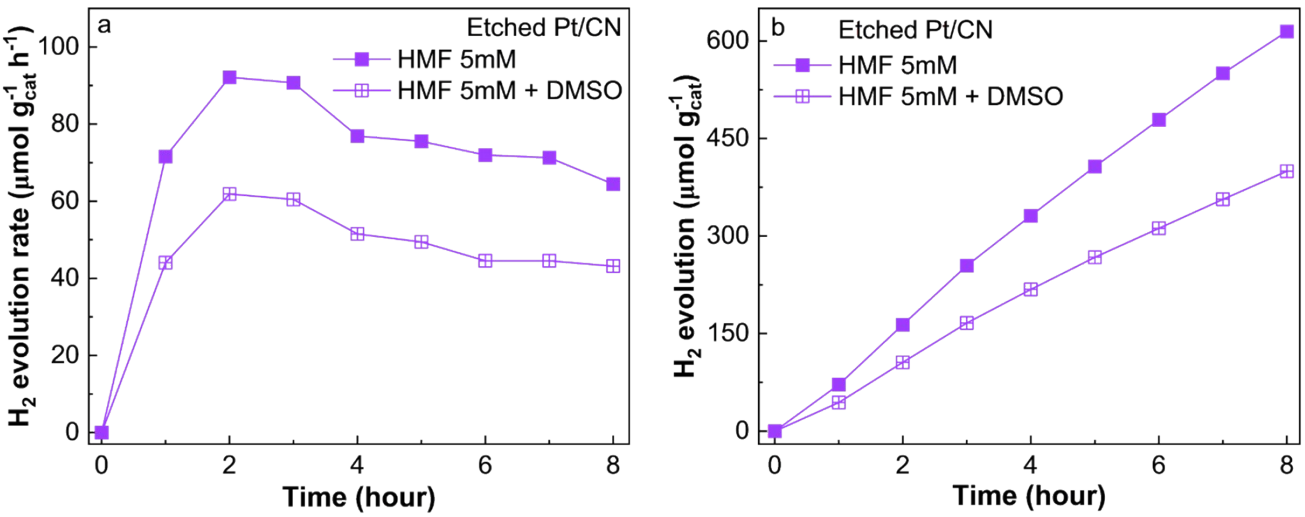

Figure S33. (a,b) Hydrogen evolution performance from HMF with and without DMSO after photoreforming tested over 8 hours. All experiments were conducted under simulated solar light conditions (AM 1.5G, 100 mW cm^{-2}, 23 ± 2 °C) utilising 100 mg of etched CN samples, with 3 wt% of Pt, reaction medium 100 ml HMF 5 mM under Ar-saturated atmosphere.

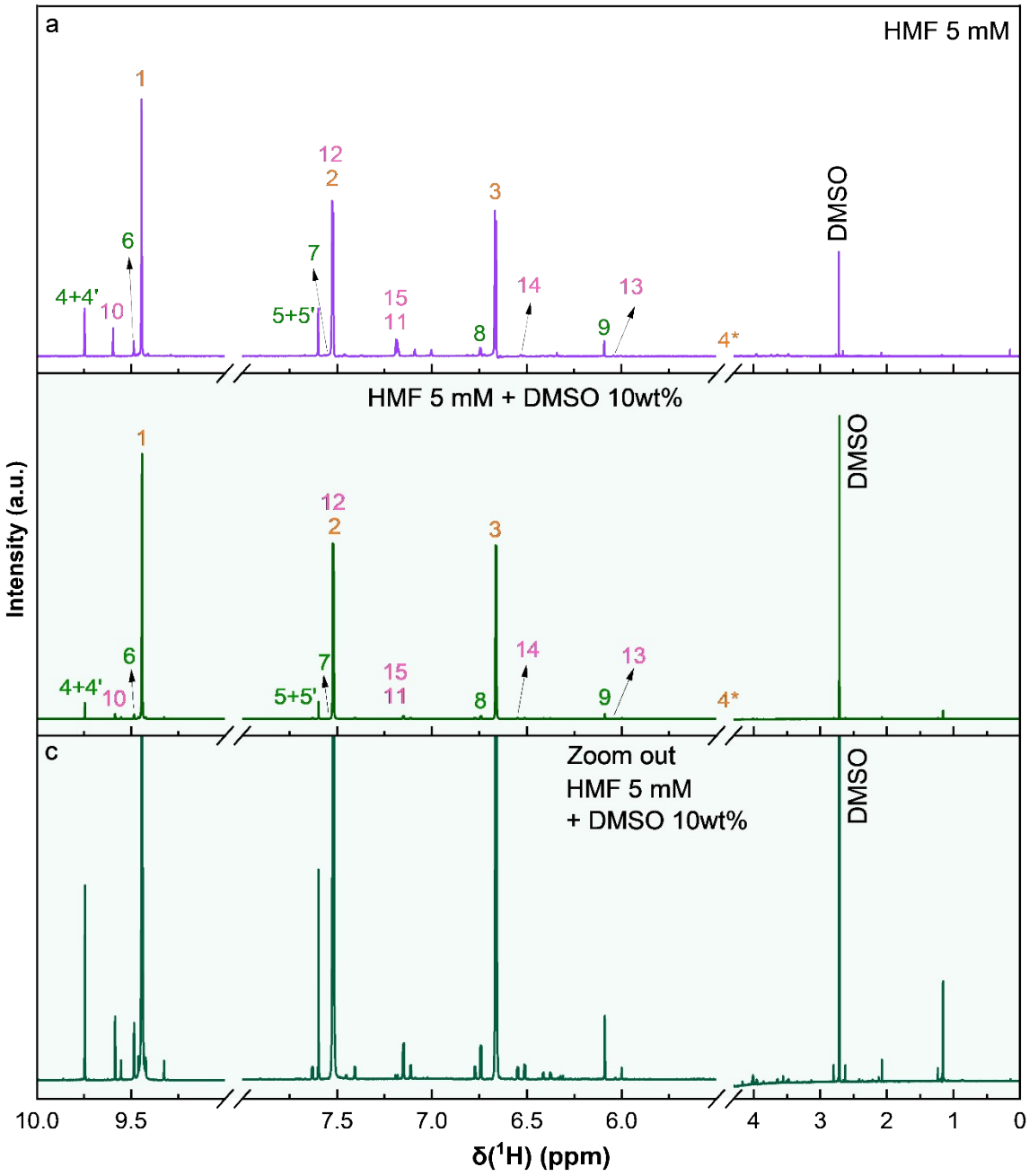

Figure S34. 1D ^{1}H NMR spectra from HMF with and without DMSO after photoreforming tested over 8 hours. All experiments were conducted under simulated solar light conditions (AM 1.5G, 100 mW cm^{-2}, 23 ± 2 °C) utilising 100 mg of etched CN samples, with 3 wt% of Pt, reaction medium 100 ml HMF 5 mM under Ar-saturated atmosphere. The two benzylic protons signal of HMF (labelled as 4* in the structure) at ~ 4.6 ppm is not shown in the spectra for clarity, as it is close to the water signal and likely suppressed due to water suppression in the 1D ^{1}H-NMR experiment.

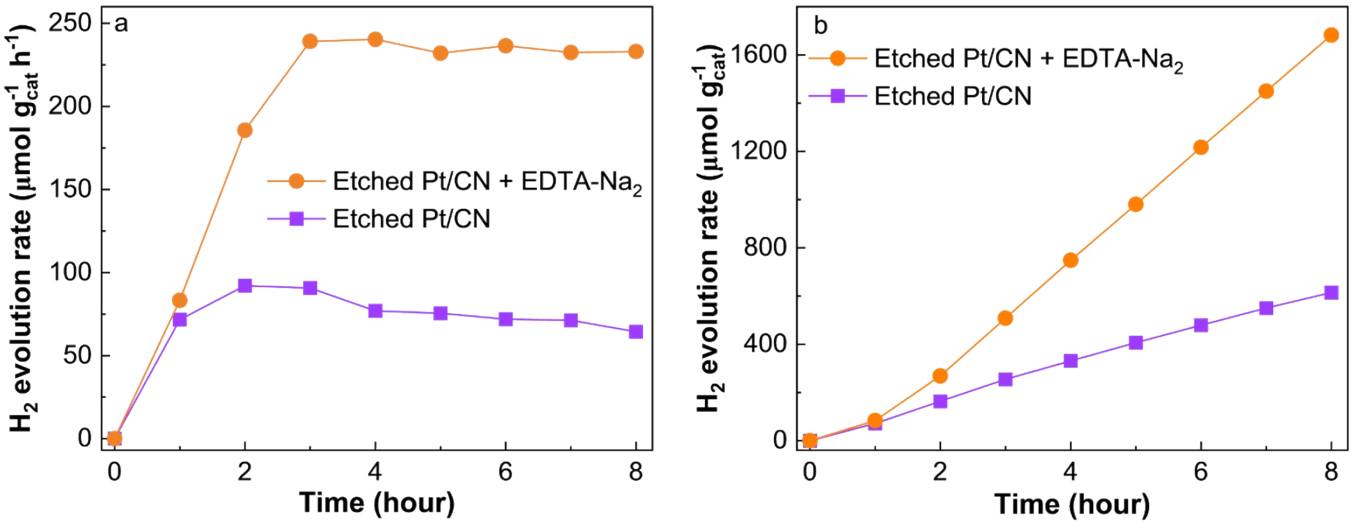

Figure S35. (a) hydrogen evolution rate and (b) the corresponding overall hydrogen yield using the etched Pt/CN photocatalyst for HMF (purple) photoreforming and HMF with addition of EDTA-Na_2 as hole scavenger (orange). Photoreaction conditions: 100 mg etched Pt/CN photocatalysts with Pt 3 wt%, 100 ml HMF 0.1 mM under simulated solar irradiation AM 1.5 G, 100 mW cm^{-2}, 23 ± 2 °C for 8 hours of photoreaction in Ar-saturated atmosphere.

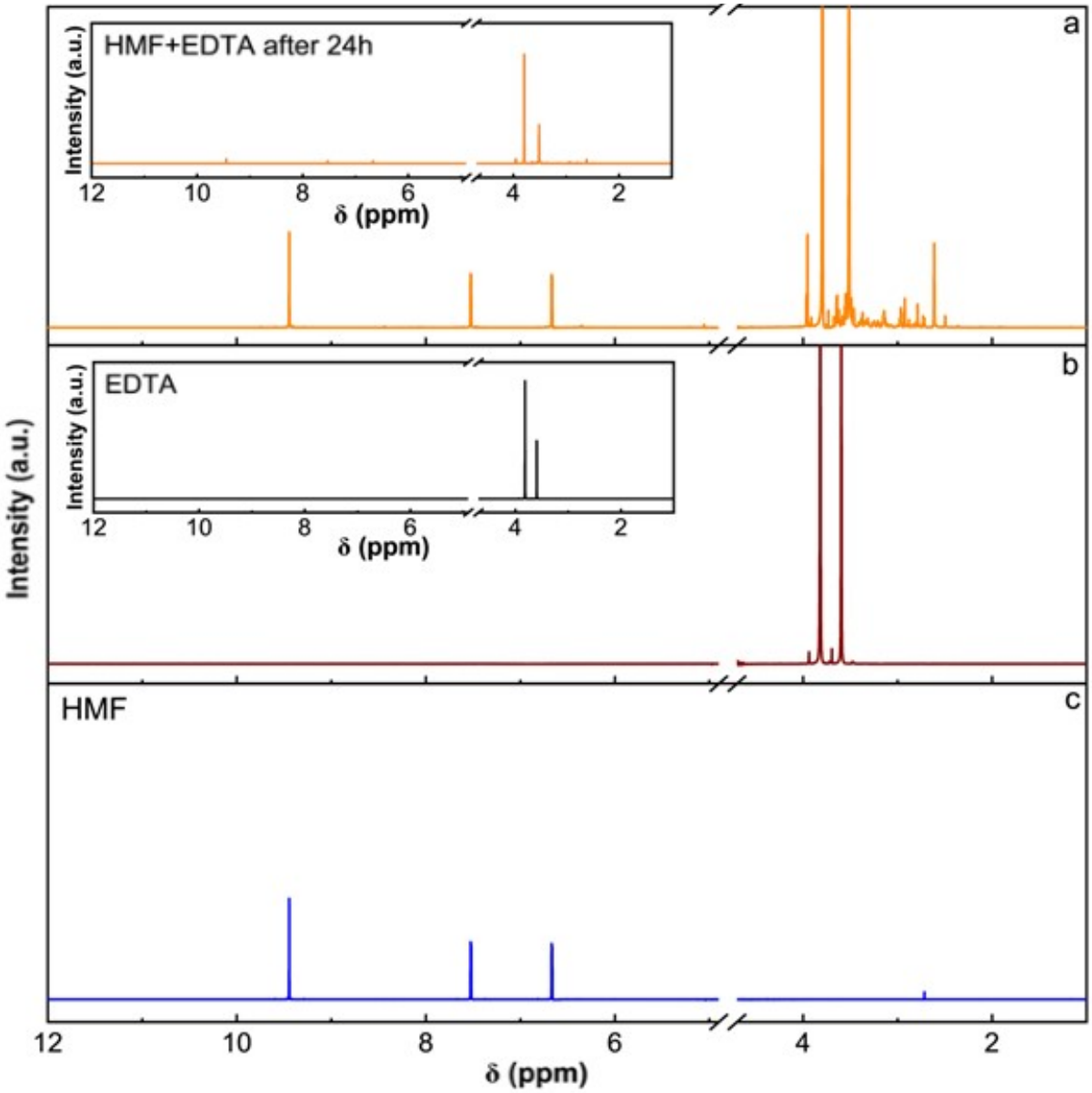

Figure S36. 1D ^{1}H NMR spectra from HMF (purple) and HMF with addition of EDTA-Na_2 photoreforming as a hole scavenger (orange). Photoreaction conditions: 100 mg etched Pt/CN photocatalysts with Pt 3 wt%, 100 ml HMF 0.1 mM under simulated solar irradiation AM 1.5 G, 100 mW cm^{-2}, 23 ± 2 °C for 8 hours of photoreaction in Ar-saturated atmosphere.

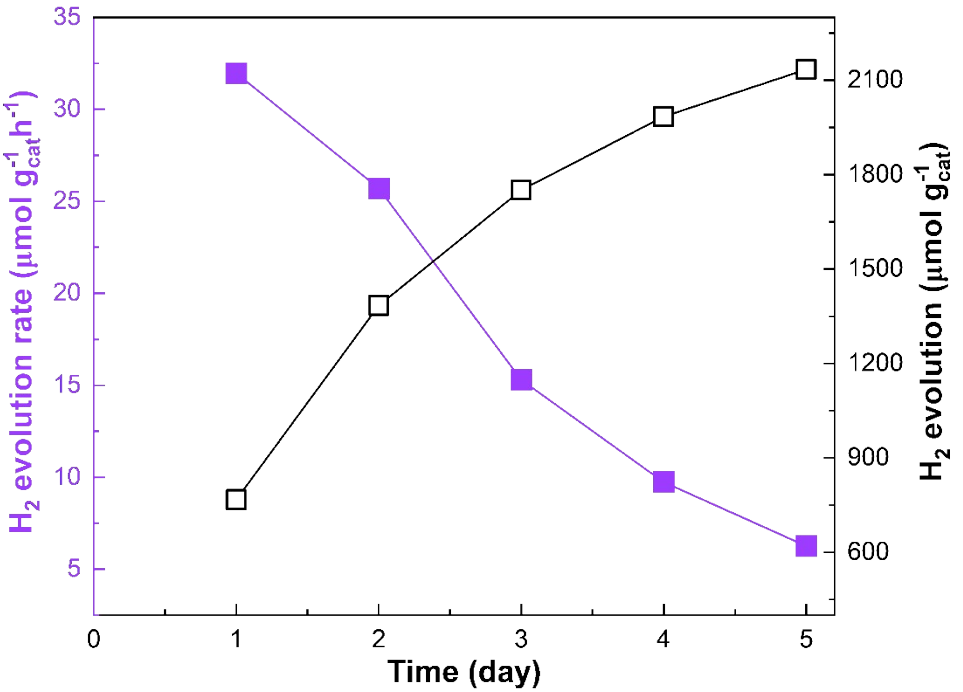

Figure S37. (a) Overall hydrogen yield and (b) the corresponding hydrogen evolution rate (measured at the 24th hour each day) during 5-day continuous photoreaction using the etched Pt/CN photocatalyst. Photoreaction conditions: 100 mg CN photocatalysts with Pt 3 wt%, 100 ml HMF 5 mM under simulated solar irradiation AM 1.5 G, 100 mW cm^{-2}, 23 ± 2 °C for 5 days of photoreaction in Ar-saturated atmosphere.

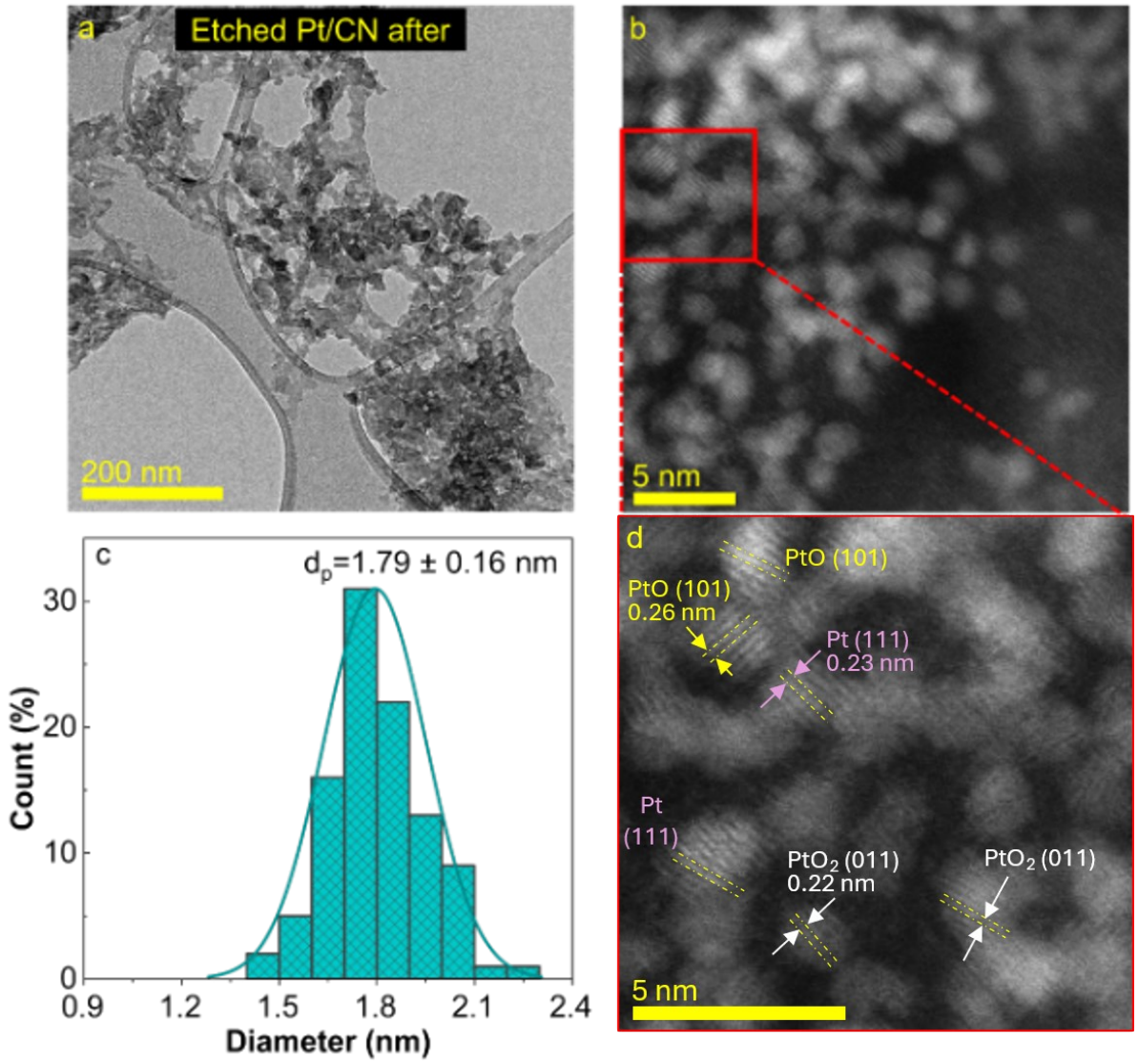

Figure S38. **TEM and HR-TEM** of etched Pt/CN after 5 days of HMF photoreforming. (a) TEM image etched Pt/CN after long-term reaction, (b,c,d) HR-TEM of platinum particles and its distribution. The observed lattice spacings of 0.23, 0.26, and 0.22 nm can be attributed to the crystallographic planes Pt(111), PtO(101), and PtO_2(011), respectively.[14,15] These values indicate the coexistence of metallic platinum and its oxidized forms, suggesting a heterogeneous distribution of Pt species, which may play a crucial role in the photocatalytic activity in 5 days. Photoreaction conditions: 100 mg CN photocatalysts with Pt 3 wt%, 100 ml HMF 5 mM under simulated solar irradiation AM 1.5 G, 100 mW cm^{-2}, 23 ± 2 °C in Ar-saturated atmosphere.

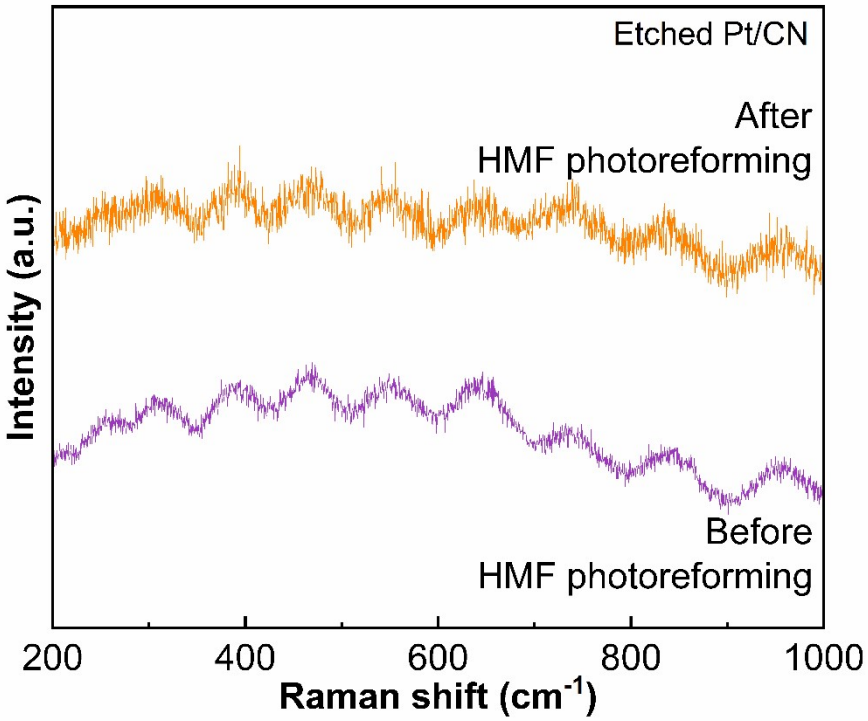

Figure S39. **Raman of etched Pt/CN after HMF photoreforming**. Photoreaction conditions: 100 mg CN photocatalysts with Pt 3 wt%, 100 ml HMF 0.1 mM under simulated solar irradiation AM 1.5 G, 100 mW cm^{-2}, 23 ± 2 °C for 24 hours of reaction in Ar-saturated atmosphere.

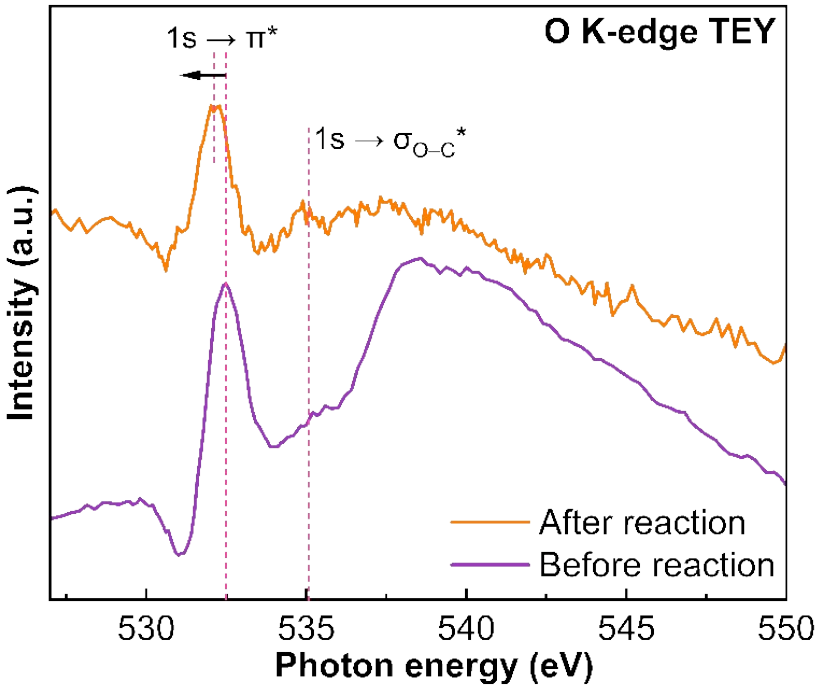

Figure S40. XAS of O K-edge of etched Pt/CN after HMF photoreforming acquired in TEY mode. Photoreaction conditions: 100 mg CN photocatalysts with Pt 3 wt%, 100 ml HMF 0.1 mM under simulated solar irradiation AM 1.5 G, 100 mW cm^{-2}, 23 ± 2 °C for 24 hours of reaction in Ar-saturated atmosphere.

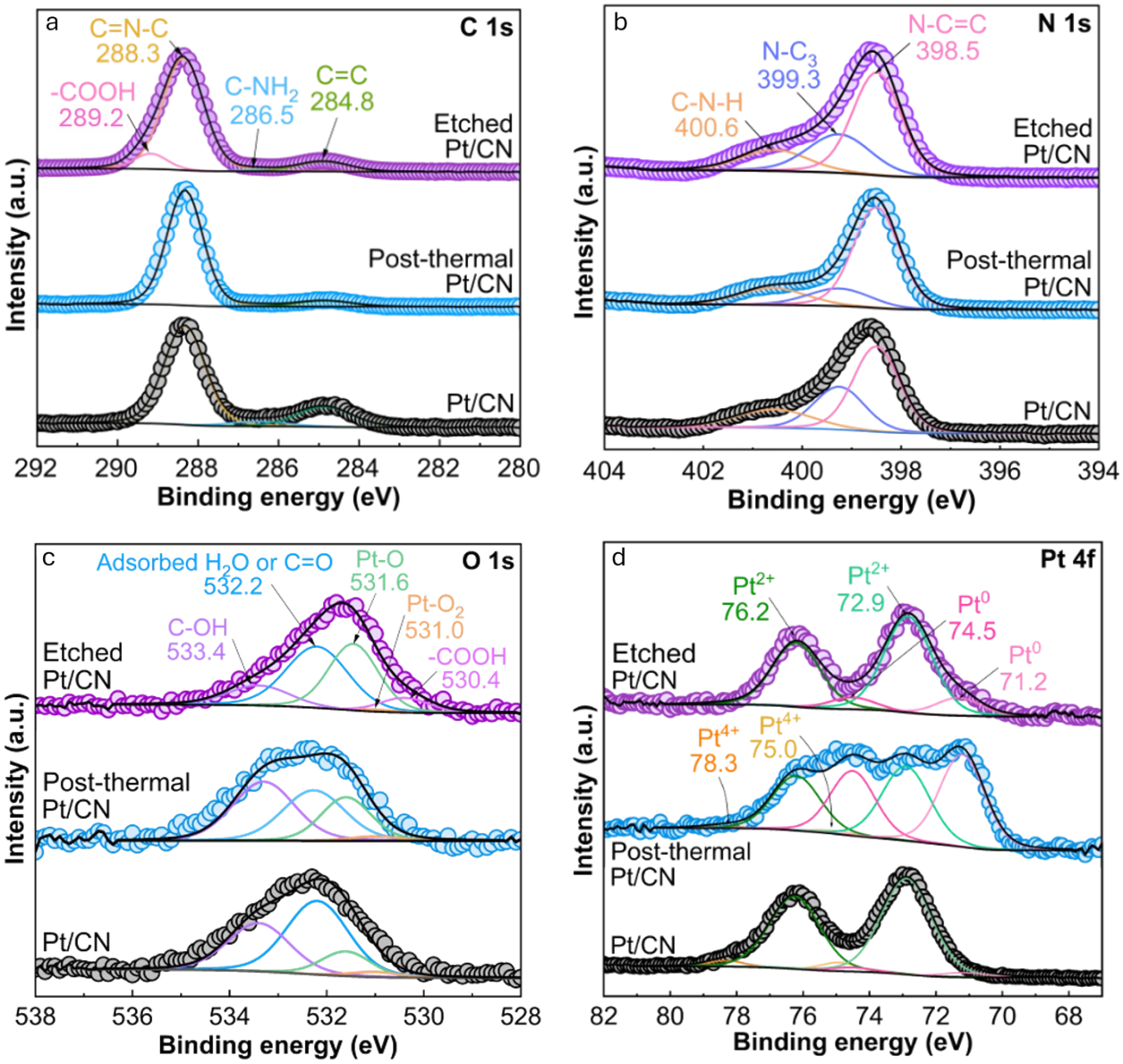

Figure S41. XPS of all photocatalysts after HMF photoreforming. Photoreaction conditions: 100 mg CN photocatalysts with Pt 3 wt%, 100 ml HMF 0.1 mM under simulated solar irradiation AM 1.5 G, 100 mW cm^{-2}, 23 ± 2 °C for 24 hours of reaction in Ar-saturated atmosphere.

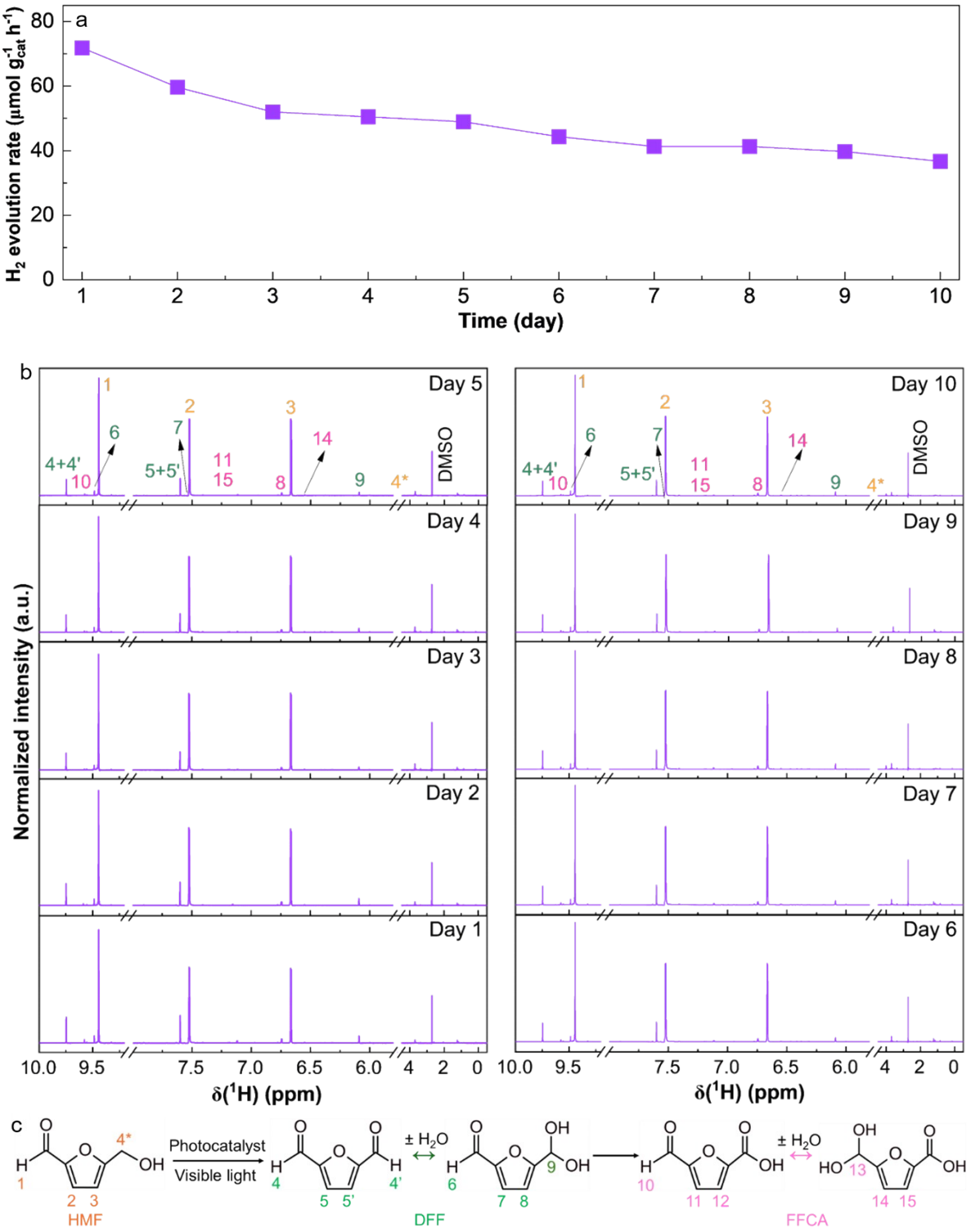

Figure S42. (a) Hydrogen evolution performance was collected at 7th hour of each day, (b) 1D ^{1}H NMR analysis of the liquid products was collected and analysis after 24 hours of photoreaction with etched Pt/CN over 10 cycles (10 days). Catalyst was recovered and fresh HMF 5 mM was added in each cycle. All experiments were conducted under simulated solar light conditions (AM 1.5G, 100 mW cm^{-2}, 23 ± 2 °C) utilising 100 mg of etched CN samples, with 3 wt% of Pt, reaction medium 100 ml HMF 5 mM under Ar-saturated atmosphere, (c) photoreforming reaction of HMF convert to DFF. The two benzylic protons signal of HMF (labelled as 4* in the structure) at ~ 4.6 ppm is not shown in the spectra for clarity, as it is close to the water signal and likely suppressed due to water suppression in the 1D ^{1}H-NMR experiment.

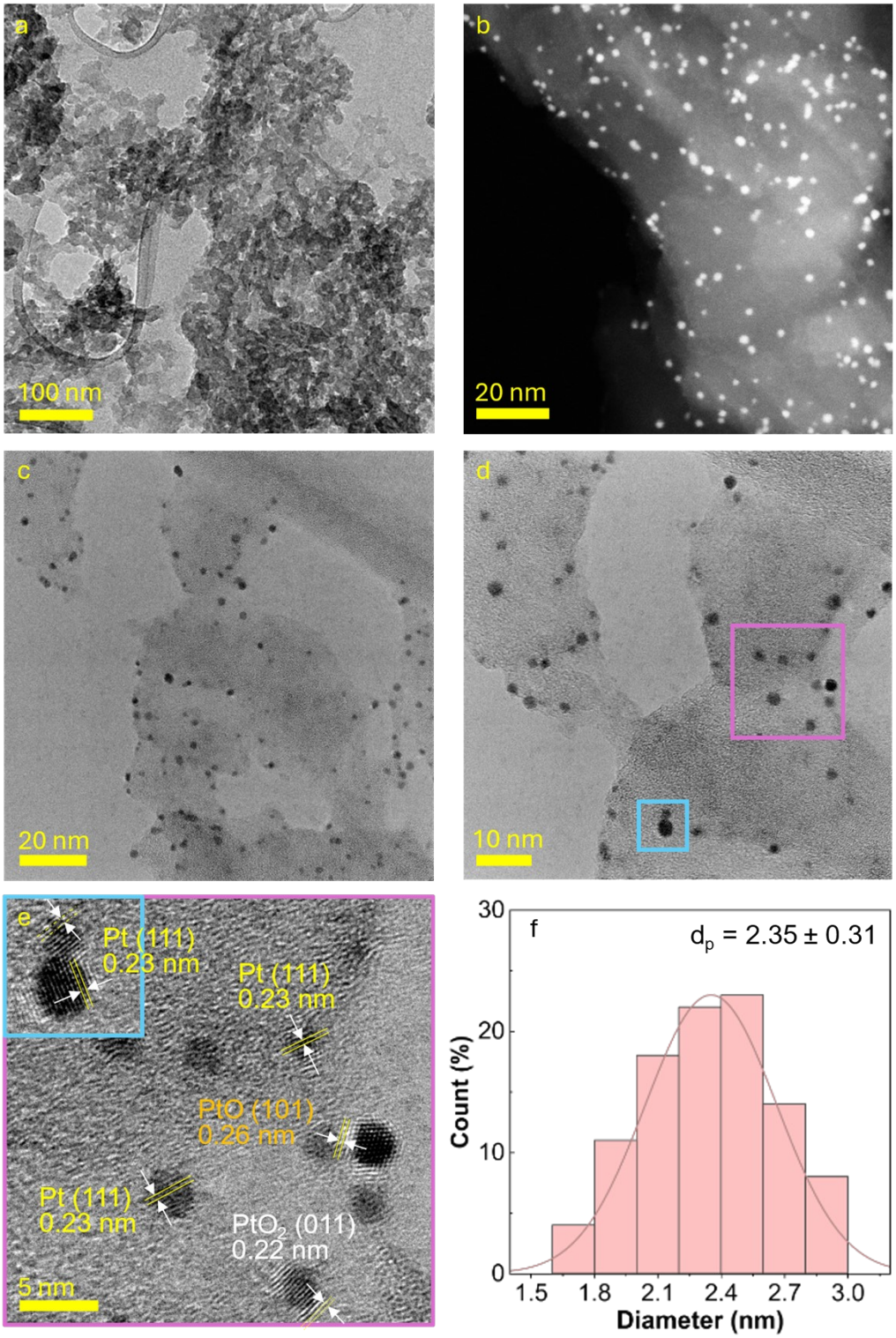

Figure S43. TEM and HR-TEM of etched Pt/CN after 10 days of HMF photoreforming. (a) TEM image of the etched Pt/CN sample after 10 days of photoreaction. (b–f) HR-TEM images of platinum nanoparticles and their distribution. The measured lattice spacings of 0.23, 0.26, and 0.22 nm correspond to the crystallographic planes of Pt(111), PtO(101), and PtO_2(011), respectively.[14,15] These findings confirm the coexistence of metallic Pt and oxidized Pt species, indicating a heterogeneous distribution of Pt states that may play a pivotal role in sustaining photocatalytic activity over the long-term reaction. Photoreaction conditions: 100 mg CN photocatalysts with Pt 3 wt%, 100 ml HMF 5 mM under simulated solar irradiation AM 1.5 G, 100 mW cm^{-2}, 23 ± 2 °C in Ar-saturated atmosphere.

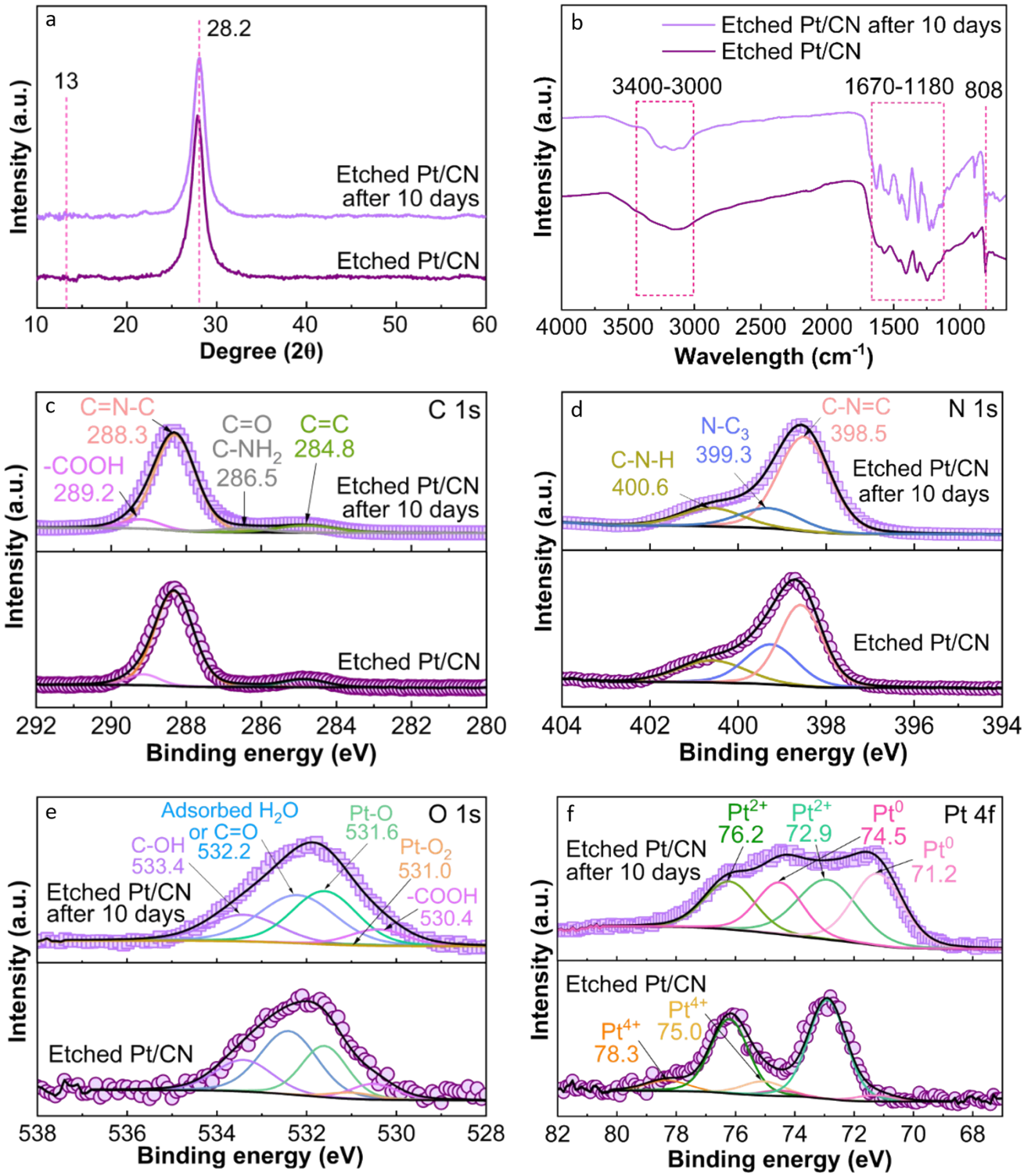

Figure S44. **X-ray diffraction and spectroscopic characterization** of *g*-C_3N_4 derived from etched Pt/CN after 10 days of HMF photoreforming**:** (a) XRD patterns, (b) FTIR, and (c-f) high-resolution XPS spectra of (d) C 1s, (e) N 1s, (e) O 1s, and (f) Pt 4f. Photoreaction conditions: 100 mg CN photocatalysts with Pt 3 wt%, 100 ml HMF 5 mM under simulated solar irradiation AM 1.5 G, 100 mW cm^{-2}, 23 ± 2 °C in Ar-saturated atmosphere.

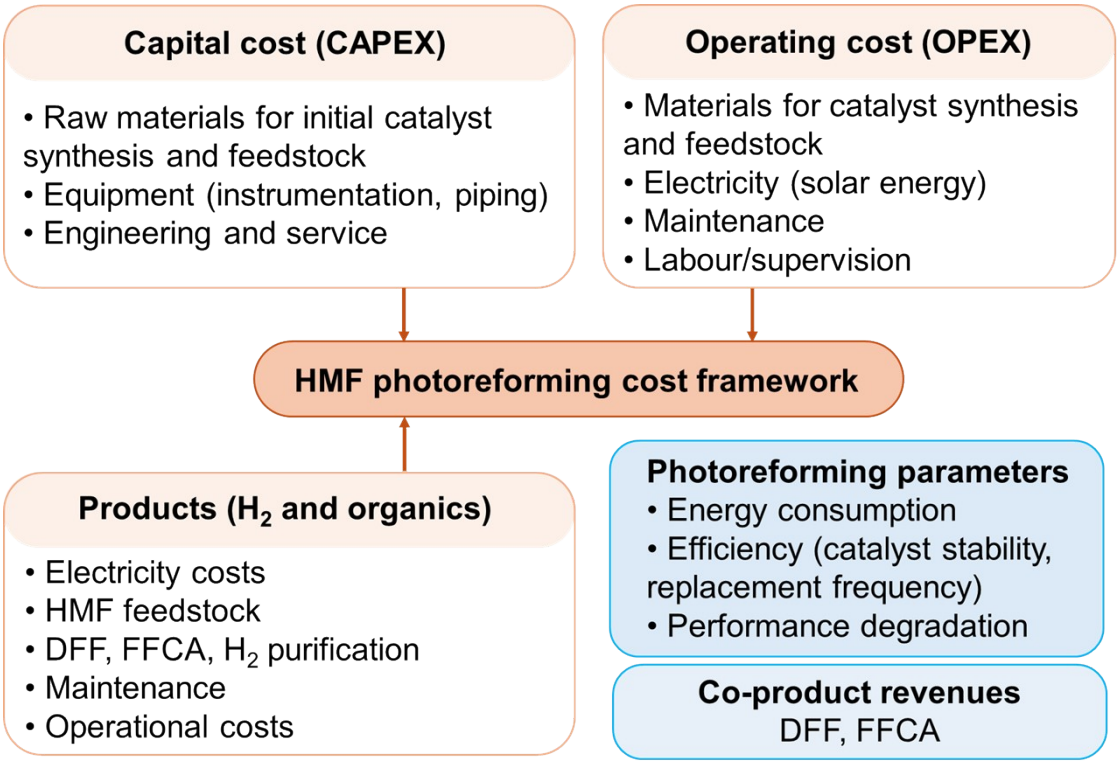

Figure S45. Flow diagram highlights the key technical and economic factors affecting levelized costs of HMF photoreforming.

Table S5. Techno-economic comparison of H_2 production technologies.

Parameter	**Our system (lab-scale) in 24 hours**[1]	**Our system (projected commercial)**	**Alkaline electrolysis**	**Proton exchange membrane (PEM) electrolysis**	**Steam ethane reforming/carbon capture and storage (SMR w/CCS)**
Performance metrics					
H_2 production rate	0.1247 $mmol_{H2}$ in 24 h	0.1185 $mmol_{H2}$ in 24 h (10 % loss)	N/A	N/A	N/A
DFF production	0.0386 $mmol_p$ in 24 h	0.03667 $mmol_p$ in 24 h (10 % loss)	N/A	N/A	N/A
FFCA production	0.0292 $mmol_p$ in 24 h	0.02774 $mmol_p$ in 24 h (10 % loss)	N/A	N/A	N/A
Energy input	Solar (direct)	Solar (direct)	48-43 kWh/kg_{H2}	54-45 kWh/kg_{H2}	Natural gas
Capacity factor	25%	35%	31-97%	31-97%	90-95%
Calculation	6 hrs sun in 24 hrs	7.2 hrs optimized in 24 h	Grid availability	Grid availability	Continuous
Annual operating hours	2,190 hrs	2,628 hrs	2,716-8,497 h	2,716-8,497 h	7,884-8,322 h
System specifications					
Catalyst Loading	100 mg (1 mg/mL)	1 kg_{cat} in total (for 100 reactors in parallel)	N/A	N/A	N/A
Reactor Volume	100 mL	1000 L in total (for 100 reactors in parallel)	N/A	N/A	N/A

HMF Concentration	5 mM	5 mM	N/A	N/A	N/A
Production calculations					
Annual H_2 Production	2.2940 g per year	305.0995 g per year	Per MW installed	Per MW installed	Per plant size
$Yield_{DFF}$	0.4371 g per year	5813.1108 g per year	N/A	N/A	N/A
$Yield_{FFCA}$	0.4159 g per year	5531.5649 g per year	N/A	N/A	N/A
Reactants	0.0631 g_{HMF} per year	630.5500 g_{HMF} per year	9 L water	9 L water	2.5 kg_{CH4}
Capital cost					
	0.1 g of catalyst need: 12 kg melamine: $1 ($110 per kg) 0.003 g platinum = ~0.008 g Chloroplatinic acid: $2 ($1300/g) Other chemicals: $50 H_2SO_4, $K_2Cr_2O_7$ Toll outsources melamine thermal processing: $3,000 Energy/lighting for loading: $3,000 Labor/facility: $20,000-30,000 **Initial Catalyst Production Cost**: $20,053 Reactor cost (design, fabrication, installation): $5,000	*1 kg of catalyst need:* 120 kg melamine: $300 ($2-4 per kg) 0.03 kg platinum = ~0.08 kg Chloroplatinic acid: $720 ($24/g) Other chemicals: $250 H_2SO_4, $K_2Cr_2O_7$ Toll outsources melamine thermal processing: $10,000 Energy/lighting for loading: $6,000 Labor/facility: $80,000-100,000 **Initial Catalyst Production Cost**: $107,270 Reactor cost (design, fabrication, installation):	N/A	N/A	N/A

		$100,000			
Equipment/chemical cost	$21,053	$207,270	$1,353,000/MW	$1,803,000/MW	$800,000/MW
CAPEX ($/kW-eq H_2)	$ 13090791.69/kW	$52542.84/kW	$1,353/kW	$1,803/kW	$800-1,200/kW
Operation costs					
Annual OPEX	$1,053	$10,364 (5 % of CAPEX)	2-4% of CAPEX	3-5% of CAPEX	2-3% of CAPEX
Catalyst regeneration	$3,210 (10 % of CAPEX)	$21,454 (20 % per year)	Industry standard	Industry standard	Industry standard
HMF Feedstock Cost/year	$1.36	$1.0719 (assuming HMF = $1700 per ton)[16]	N/A	N/A	Natural gas cost
Total Annual Operating Cost	$4,265	$31,819	$445,000-670,000	$550,000-820,000	$250,000-400,000
Co-product revenues					
DFF Revenue @ $10,480/kg (lab)	$1,997	N/A	N/A	N/A	N/A
FFCA Revenue @ $8,600/kg (lab)	$1,559	N/A	N/A	N/A	N/A
DFF Revenue @ $100/kg (industrial)	N/A	$1,905	N/A	N/A	N/A

FFCA Revenue @ $150/kg (industrial)	N/A	$2,720	N/A	N/A	N/A
Total Co-product revenue	$3,556	$4,625	$48,000 ($O_2$)	$48,000 ($O_2$)	-$50/tonne CO_2
Annualized CAPEX	$2,145	$21,121	$137,861/MW	$183,696/MW	$81,520/MW
LCOH - H_2 only ($/kg)	**$10,112.68**	**$748.58**	$4.5-6.5[17]	$5.0-7.0	$1.93[18]
LCOH - with Co-products ($/kg)	**$8,562.55**	**$733.42**	$4.5-6.5	$5.0-7.0	$1.93[18]

[1]Calculated based on the HMF photoreforming performance utilising 100 mg of etched CN sample, with 3 wt% of Pt. Experimental simulated solar light (AM 1.5G, 100 mW cm^{-2}, 23 ± 2 °C) reaction medium 100 ml HMF 5 mM under Ar-saturated atmosphere.

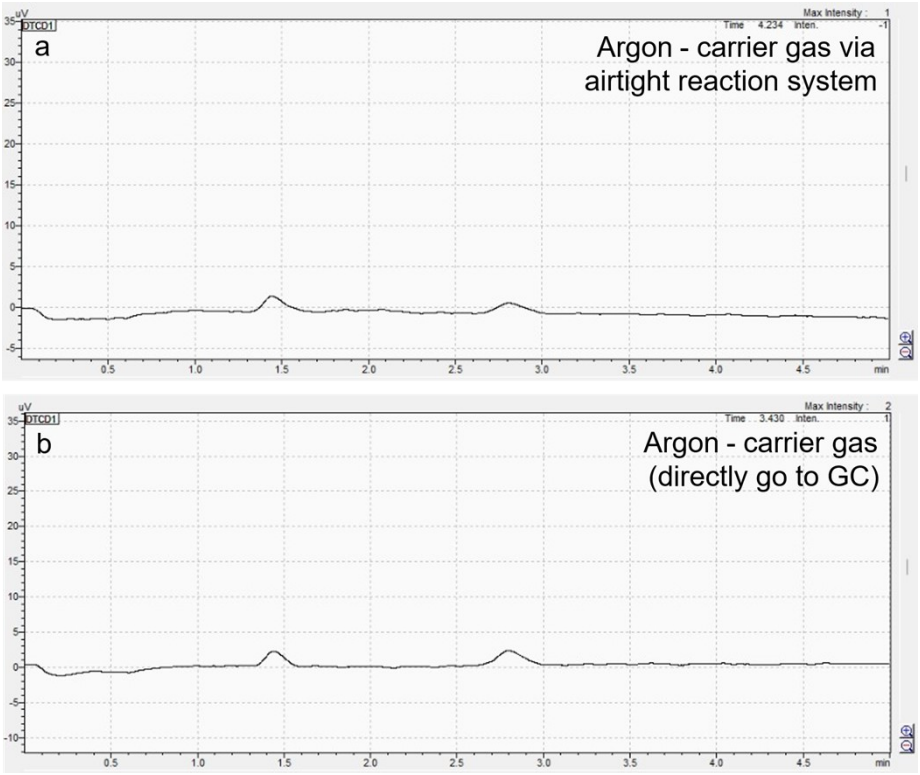

Figure S46. Chromatogram view of gas samples obtained from GC analyses of (a) Ar gas as a carrier gas (gas flow 20 cc min^{-1}) going through a sealed reactor system before starting the photoreforming reaction, (b) Ar was directly connected to GC. There are no H_2 is detected.

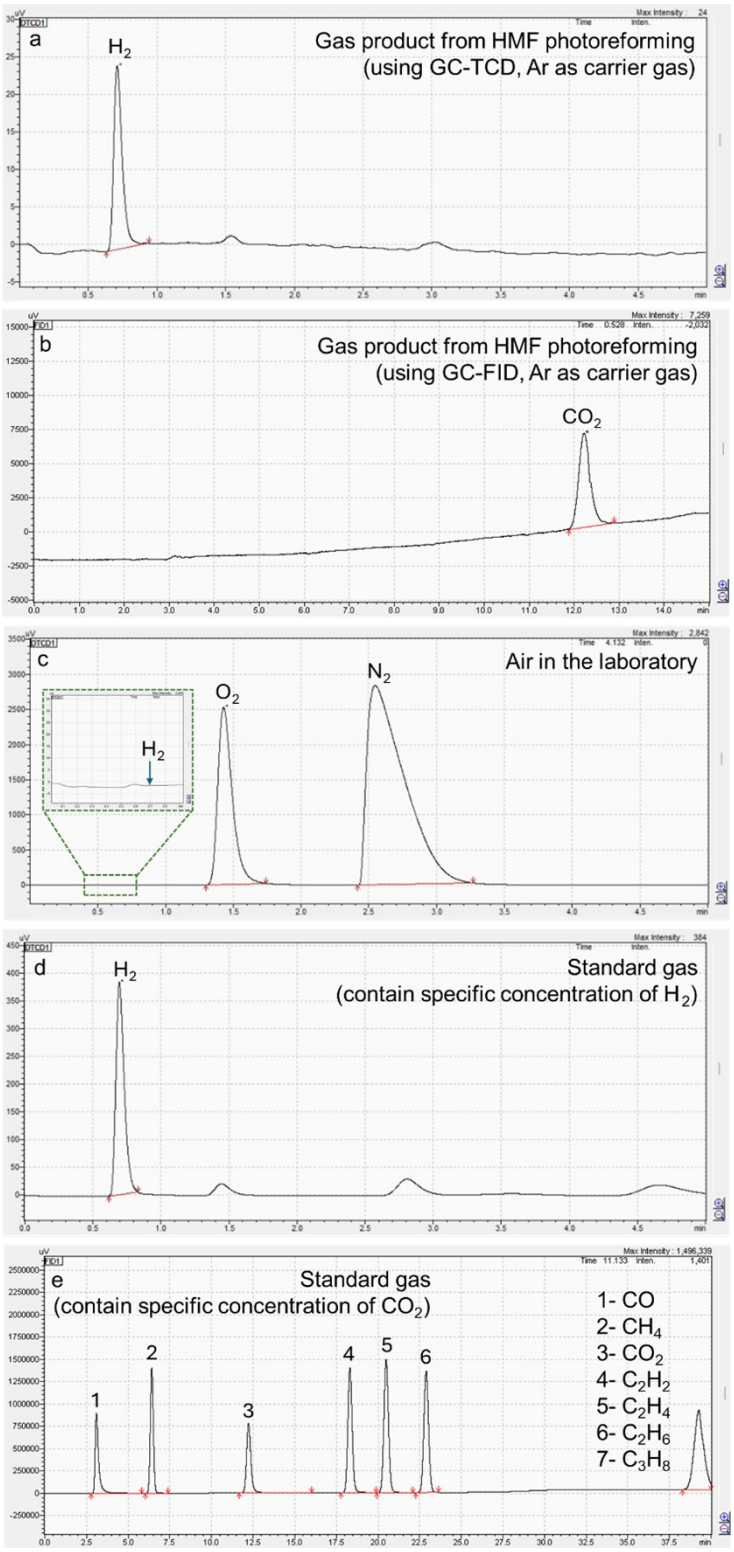

Figure S47. Chromatogram view of samples obtained from GC analyses: gas product from HMF photoreforming via (a) a thermal conductivity detector (TCD), (b) A flame ionization detector (FID) using etched Pt/CN recorded at the 7th hour. Experimental simulated solar light (AM 1.5G, 100 mW cm^{-2}, 23 ± 2 °C) utilising 100 mg of etched CN sample, with 3 wt% of Pt, reaction medium 100 ml HMF 5 mM under Ar-saturated atmosphere. (c) Air components at laboratory, (d) standard gas mixture containing 0.1958 %(mol/mol) H_2 in Ar carrier gas (Sourced from Coregas Australia Supplier), the H_2 peak is located at 0.695 min. (e) Standard gas mixture containing 0.2098 %(mol/mol) CO_2 (Sourced from Coregas Australia Supplier), the CO_2 peak is located at 12.242 min.

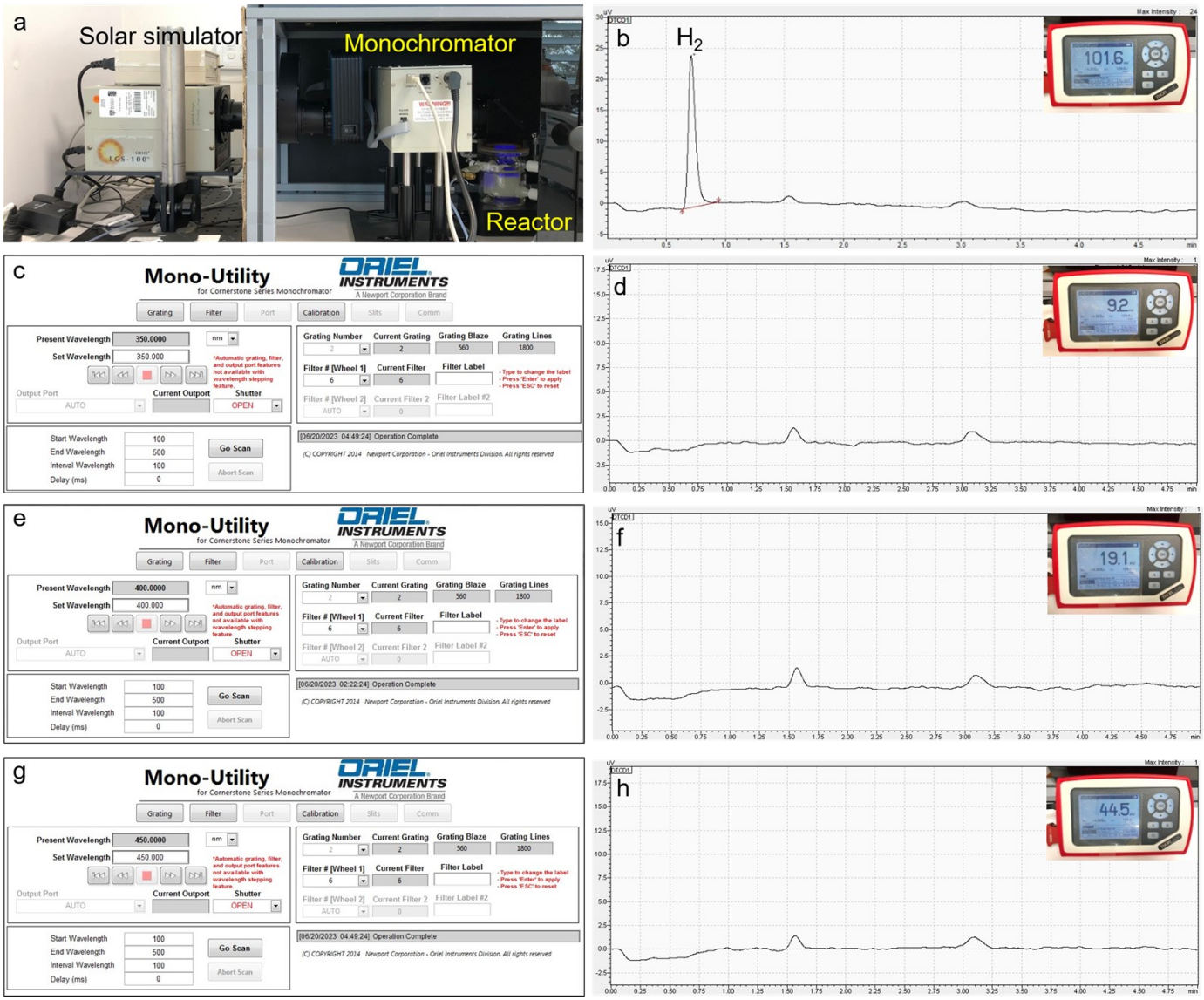

Figure S48. Quantum efficiency of H_2 evolution: (a) A solar simulator (Oriel LCS-100™, Newport, US) equipped with a monochromator (Oriel Cornerstone 130 1/8 m monochromator and a motorized filter wheel (USFW-100, Newport, US)) setup. (b) Light intensity measurement equipment (Thorlabs GmbH, PM100D, Germany) placed at the liquid|air interface under full range irradiation with corresponding GC spectrum. (c-h) The wavelength input, the obtained light intensity and GC spectrum for H_2 detection corresponding for wavelength at 350 nm (c, d), 400 nm (e, f) and 450 nm (g, h). Experimental simulated solar light (AM 1.5G, 100 mW cm^{-2}, 23 ± 2 °C) utilising 100 mg of etched CN sample, with 3 wt% of Pt, reaction medium 100 ml HMF 5 mM under Ar-saturated atmosphere.

References

[1] J. Moulder, W. Stickle, P. Sobol, K. Bomben, *Perkin-Elmer Corpor.* 1992, 260.

[2] A. Mehtab, S. A. Ali, P. P. Ingole, Y. Mao, S. M. Alshehri, T. Ahmad, *ACS Appl. Energy Mater.* 2023, *6*, 12003.

[3] "Nickel | Periodic Table | Thermo Fisher Scientific - AU," can be found under https://www.thermofisher.com/au/en/home/materials-science/learning-center/periodic-table/transition-metal/nickel.html, n.d.

[4] A. A. Rosatella, S. P. Simeonov, R. F. M. Frade, C. A. M. Afonso, *Green Chem.* 2011, *13*, 754.

[5] H. Ojagh, A. Achour, P. H. Ho, D. Bernin, D. Creaser, O. Pajalic, J. Holmberg, L. Olsson, *React Chem. Eng.* 2021, *7*, 192.

[6] Z. Bi, X. Cui, H. Xu, Q. Li, D. Xu, Y. Guo, *Chem. Eng. J.* 2025, *510*, 161613.

[7] Y. Román-Leshkov, C. J. Barrett, Z. Y. Liu, J. A. Dumesic, *Nature* 2007, *447*, 982.

[8] D. M. Alonso, S. G. Wettstein, J. A. Dumesic, *Green Chem.* 2013, *15*, 584.

[9] C. Moreau, A. Finiels, L. Vanoye, *J. Mol. Catal. A Chem.* 2006, *253*, 165.

[10] H. Zhao, J. E. Holladay, H. Brown, Z. C. Zhang, *Science* 2007, *316*, 1597.

[11] D. Cruz, H. Park, P. Tiller, R. Gonzalez, A. Mittal, D. K. Johnson, S. Park, *J. Environ. Chem. Eng.* 2025, *13*, 116069.

[12] J. N. Chheda, Y. Román-Leshkov, J. A. Dumesic, *Green Chem.* 2007, *9*, 342.

[13] N. Thanheuser, L. Schlichter, W. Leitner, J. Esteban, A. J. Vorholt, *RSC Sustain.* 2025, *3*, 1848.

[14] M. Wang, Y. Liu, D. Li, J. Tang, W. Huang, *Chinese Chem. Lett.* 2019, *30*, 985.

[15] X. Yang, Y. Li, P. Zhang, R. Zhou, H. Peng, D. Liu, J. Gui, *ACS Appl. Mater. Inter.* 2018, *10*, 23154.

[16] A. H. Motagamwala, K. Huang, C. T. Maravelias, J. A. Dumesic, *Energy Environ. Sci.* 2019, *12*, 2212.

[17] "Hydrogen Insights 2023 December Update | Hydrogen Council" can be found under https://hydrogencouncil.com/en/hydrogen-insights-2023-december-update/, n.d.

[18] "H2A: Hydrogen Analysis Production Models | Hydrogen and Fuel Cells | NREL," can be found under https://www.nrel.gov/hydrogen/h2a-production-models, n.d.